

Matteo Fomolli

Optimization of solar energy use with a dynamic integrated photovoltaic shading device

Master's thesis in Sustainable Architecture

Supervisor: Gabriele Lobaccaro, Francesco Goia, Ellika Taveres-Cachat

June 2020

NTNU
Norwegian University of Science and Technology
Faculty of Architecture and Design
Department of Architecture and Technology



Norwegian University of
Science and Technology

Matteo Fomolli

Optimization of solar energy use with a dynamic integrated photovoltaic shading device

Master's thesis in Sustainable Architecture

Supervisor: Gabriele Lobaccaro, Francesco Goia, Ellika Taveres-Cachat
June 2020

Norwegian University of Science and Technology
Faculty of Architecture and Design
Department of Architecture and Technology

Abstract

The integration of photovoltaics on the buildings' envelopes is getting increasing attention in the last few decades. Stringent energy regulations have led to the development of new products, responding to multiple functions simultaneously. This thesis investigates the potential of photovoltaic integrated shading devices (PVSDs), by proposing a methodology to assess the advantages of a dynamic shading system over a static one, for different time characterisations and latitudes. The optimisation is carried out through a multi-objective optimisation (MOO) approach, having as objectives the reduction of total energy consumption and an adequate level of internal natural daylight. A simple office room, with the shading devices installed on the two south-oriented windows, is used as test geometry to perform the analysis. The study demonstrates an overall improvement at every latitude by adopting a dynamic system, especially when the frequency of changes in the orientation of the system increase along the year. The most remarkable results are visible at lower latitudes, where levels of optimisation higher than 20% are obtained. The entire study, from the geometry creation to the energy and daylight simulations, was conducted inside the Grasshopper environment, using the Ladybug Tools as software packages. The final aim of the thesis is to contribute to broadening the potentialities on PVSDs, as well as drawing general outlines, valid when considering the adoption of a dynamic system of this kind.

Sammendrag

Integrasjon av solceller på bygningskroppen har fått stadig økende oppmerksomhet de siste tiårene. Strengere krav til energieffektivitet har fremmet utviklingen av nye produkter, som har mulighet til å løse flere problemer samtidig. Denne masteravhandlingen skal ta for seg potensialet ved bruk av solceller med integrerte solavskjerming(PVSDs), ved å foreslå en metode som kan vurdere fordeler ved bruk av dynamisk solavskjerming fremfor statisk. Analysene vil bli foretatt for forskjellige tidskarakteriseringer i tillegg til lokasjoner med ulik breddegrad. Optimaliseringen gjennomføres gjennom en MOO-tilnærming (multi-objective optimisation), der målet er å redusere totalt energiforbruk og at samtidig tilstrekkelig dagslys blir opprettholdt. Testene er gjennomført i et enkelt kontor med solavskjermings anordning på to vinduer som er orientert mot sør. Resultatet fra studien viser en generell forbedring for alle breddegrader ved bruk av et dynamisk system, spesielt der det er økning i tidskarakteristikken gjennom året. Funnene som vekker størst oppsikt er ved lavere breddegrader, der nivået på optimaliseringen kan nå opp mot 20%. Simuleringsprogrammet Ladybug for Grasshopper har blitt benyttet, fra geometriskapning til energisimuleringer. Målet med denne masteravhandlingen har vært å åpne opp for vider utvikling for PVSDs, samt undersøke hovedtrekkene ved å ta i bruk dynamiske systemer.

Table of Contents

Abstract	1
Sammendrag	2
Table of Contents	3
List of Tables	5
List of Figures	6
Abbreviations	7
1 Introduction	8
1.1 Aim of the thesis	10
1.2 Thesis outline	10
2 Background	11
2.1 Building Integrated Photovoltaics	11
2.1.1 Advantages of Photovoltaic Shading Devices	11
2.1.2 Optimal Materials for Photovoltaics Integration in Shading Devices	13
2.2 Parametric design	13
2.2.1 Grasshopper: an open source visual language for architects	14
2.3 Ladybug tools	14
2.4 Daylight simulations	15
2.4.1 Light ray-tracing technique as a base for simulations	15
2.4.2 The Daylight Coefficients Method	16
2.4.3 Complex fenestration surfaces simulation problems	17
2.4.4 Bidirectional Scattering Distribution Functions: a solution for CFS	17
2.4.5 Limitations of Daylight Coefficients Method	18
2.4.6 The Three-Phase Method	19
2.5 A new plug-in for advanced users: Honeybee [+]	20
3 Methodology	21
3.1 Geometry Description	24
3.2 PV Settings	24
3.3 Energy settings	25
3.4 Daylight settings	27
3.5 Electric light settings	29
3.6 Objectives functions of the optimisation	30
3.7 Selected geographical locations	30
3.8 Multi-objective optimisation process	32

4	Results and discussion.....	35
4.1	Oslo.....	35
4.1.1	Oslo Adiabatic.....	37
4.1.2	Oslo 13 and 10 louvres.....	38
4.2	Brussels.....	39
4.3	Rome.....	40
4.3.1	Rome 13 and 10 louvres.....	41
4.4	Cairo.....	42
4.4.1	Cairo 19 louvres.....	44
4.5	Limitations of the study	44
5	Conclusion	46
5.1	Further developments	47
	Bibliography.....	48

List of Tables

Table 1. Thermal properties of the envelope and technical systems; adapted from Taveres-Cachat et al., 2019255	
Table 2. Optical properties of the surfaces used in the model	277
Table 3. Layers composing the complex fenestration system; T_{sol} : solar transmittance, R_{sol1} : solar reflectance exterior facing side, R_{sol2} : solar reflectance interior facing side, T_{vis} : visible transmittance, R_{vis1} : visible reflectance exterior facing side, R_{vis2} : visible reflectance interior facing side	288
Table 4. Radiance settings for the daylight simulation, the lower option was chosen; -ab: ambient bounces, -ad: ambient divisions, -as: ambient sampling, -aa: ambient accuracy, -ar: ambient resolution	29
Table 5. Overview of the four analysed locations with the number of louvres tested; in red is underline the 16 louvres configuration, which was the main focus of the study * for this specific location and configuration a series of simulations with adiabatic surfaces were also tested	311
Table 6. Overview of the optimisation of a dynamic system over a static one for Oslo 16 louvres.....	36
Table 7. Influence of thermal history when the settings of the exterior surfaces are changed from facing the exterior to adiabatic.....	37
Table 8. Overview of the optimisation of a dynamic system over a static one for Oslo 16 louvres adiabatic	37
Table 9. Overview of the optimised results for 13 and 10 louvres configurations in Oslo and the percentage difference to the 16 louvres configuration for cDA and E_{TOT}	38
Table 10. Overview of the optimisation of a dynamic system over a static one for Brussels.....	39
Table 11. Overview of the optimisation of a dynamic system over a static one for Rome 16 louvres	41
Table 12. Overview of the optimised results for 13 and 10 louvres configurations in Rome and the percentage difference to the 16 louvres configuration for cDA and E_{TOT}	41
Table 13. Overview of the optimisation of a dynamic system over a static one for Cairo 16 louvres	43
Table 14. Overview of the optimisation of a dynamic system over a static one for Cairo 19 louvres	44

List of Figures

Fig. 1. Chart of publications in the last twenty years with PVSD as topic; image from Zhang et al., 2018	9
Fig. 2. A PVSD product by the company SolarGaps installed in the World Trade Center office building in Barcelona (Spain) (SolarGaps, 2020)	12
Fig. 3. Representation of the backward raytracing method; image credits: Ivensen et al., 2013.....	15
Fig. 4. Schematic diagram of the Daylight Coefficients Method; image credits: Reinhart, 2001	16
Fig. 5. Representation of interior and exterior vectors of a BSDF; image credits: Fernandes, 2006	18
Fig. 6. Comparison between the Daylight Coefficients (left), and the Three-Phase (right) methods; image credits: Subramaniam, 2017.....	19
Fig. 7. Simple decision tree to select the best simulation according to geometry and objectives of the study; image credits: Mostapha Sadeghipour Roudsari	21
Fig. 8. Flowchart summary of the design methodology	22
Fig. 9. Visualisation of the workflow developed in the Grasshopper environment.....	23
Fig. 10. Views of the geometry of the Bestest Case 600 in Rhinoceros 3D environment.....	24
Fig. 11. Honeybee_EnergyPlus Window Shade Generator component.....	26
Fig. 12. Strings of the Honeybee_EnergyPlus Window Shade Generator component to edit in order to set a SlatAngle schedule; the specific syntax to change in lines 1123 and 1127 is highlighted.....	27
Fig. 13. Diagram of the total illuminance recorded at the test point for one year in Oslo with a 16 louvres system at 0° (upper image) and the electric light schedule which compensates proportionally and keeps the overall daylight value over 500 lux.....	29
Fig. 14. Summary of the data processed throughout the simulation	31
Fig. 15. Chart representing the quadratic trend of the E_{TOT} of the month of July in Oslo for a configuration with 16 louvres; in red is highlight the lower value picked, which correspond at the vertex of the parabola	33
Fig. 16. Diagram showing the passages for the creation of a definitive monthly schedule for Oslo with a configuration of 16 louvres. The boxes with numbers represent the angles to test for every month since they guarantee a cDA level above 50%; the darker blue indicates the best configuration according to the preliminary analysis while the light blue the shows the simulations actually run, taking in consideration the quadratic distribution of the E_{TOT} results	34
Fig. 17. Chart showing the Oslo 16 louvres share of energy and cDA for the different configurations of the photovoltaic shading device	35
Fig. 18. Chart illustrating angles' alternation for seasonal, monthly, and weekly schedules for Oslo 16 louvres	357
Fig. 19. Illustration showing the reduction in PV area by diminishing the number of louvres	35
Fig. 20. Chart showing the Brussels share of energy and cDA for the different configurations of the photovoltaic shading devices	39
Fig. 21. Chart showing the Rome 16 louvres share of energy and cDA for the different configurations of the photovoltaic shading device	40
Fig. 22. Chart showing the Cairo 16 louvres share of energy and cDA for the different configurations of the photovoltaic shading device	42
Fig. 23. Chart illustrating angles' alternation for seasonal, monthly and weekly schedules for Cairo 16 louvres	424

Abbreviations

PVSD	Photovoltaic Shading Device
MOO	Multi-Objective Optimization
BIPV	Building Integrated Photovoltaic
ZEB	Zero Emission Building (Research center)
PV	Photovoltaic
EU	European Union
a-Si	Amorphous Silicon (cells)
CdTe	Cadmium Telluride (cells)
CIGS	Copper Indium Gallium Selenide (cells)
EPW	Energy Plus Weather (file)
DC	Daylight Coefficients (method)
TMY	Typical Meteorological Year
CFS	Complex Fenestration Surface
BSDF	Bidirectional Scattering Distribution Function
LBNB	Lawrence Berkeley National Laboratories
V	View matrix
T	Transmission matrix
D	Daylight matrix
S	Sky matrix
E_{TOT}	Total annual net energy use
cDA	Continuous daylight autonomy

1 Introduction

It is estimated that people spend approximately 90% of their lifetime indoors (Klepeis et al., 2001), a fact which underlines the importance of guaranteeing adequate levels of indoor thermal and visual comfort in buildings. Additionally, buildings are responsible for nearly one-third of the world energy consumption, making them the second most energy-intensive sector of the market (IEA, 2020) and one with a significant potential for improvement. This is even more evident if referring to office buildings, a category that in the last century, with the advent of the modern style in architecture, have seen the extensive use of glazed facades (Bizzarri et al., 2011).

These transparent envelopes have significantly lower insulation properties compared to opaque building material, making these buildings strictly dependant from technical systems for cooling, heating, ventilation and artificial lighting, with consequent high energy demand (Karkanias et al., 2010). In this context, technological solutions which can positively impact indoor thermal and visual comfort, as well as energy consumption, are particularly interesting to develop and implement. The integration of photovoltaics into buildings (BIPV) can, therefore, be seen as a viable solution also thanks to the rapid technological improvements in panels' efficiency experienced in the last decade.

Due to the double function that can provide, serving as electricity generators and simultaneously substitute a building component, their use is expected to become progressively relevant in meeting the increasingly stringent energy regulations. If taking the European Union as a reference case, by 2020 all newly constructed buildings are supposed to be nearly zero energy, while in Norway the Research Centre for Zero Emission Buildings (ZEB) has taken a step further by aiming for a net-zero balance for the lifespan of new buildings (Hestnes and Eik-Nes, 2017). These daring goals would be impossible to be achieved without imagining an on-site production of energy through the use of integrated photovoltaics.

Among the wide varieties of available technologies, the integration of photovoltaics into shading devices (PVSD) has proven to be particularly promising, addressing two problems at the same time. The unwanted solar radiation is converted into energy directly in situ instead of being reflected away as for a standard system, avoiding internal overheating, and the visible light is filtrated according to optimal visual comfort.

Previous studies have shown the possibilities of improvement in visual comfort coupled with a reduction in energy use both for fixed (Hassan et al., 2017; Mandalaki et al., 2014, 2012; Taveres-Cachat et al., 2019, 2017) and dynamic systems (Abdullah and Alibaba, 2017; Gao et al., 2018; S. Hong et al., 2017; Hong et al., 2016; Ibraheem et al., 2020; Kim et al., 2010).

Despite that, the optimal solution always depends on many factors such as location, orientation, climatic conditions, building function, efficiency as well as geometry and blinds control strategies. The complexity in designing an optimal solution for PVSDs resides in the challenging task of balancing the uses of solar energy. The optimisation of PV production or the shield of solar radiation to cool down the building can lead to a poorly daylight environment, while the need for optimal daylight levels can result in overheating problems and low energy production by the system. Therefore, it is necessary to account for all these competing parameters to have a product able to perform better than its counterpart without PV or just the simple window (Alzoubi and Al-Zoubi, 2010; Mandalaki et al., 2012).

The attention of the market for integrated photovoltaic is progressively increasing in the last few decades, and their use is expected to provide more than the 20% of the energy need in the EU 27 by 2030 (Defaix et al., 2012). However, PVSDs still experience obstacles for a full development that were underlined by Zhang et al. (2018) as outcomes of meticulous research. The main limitations are pointed as a reduced body of knowledge that yet characterises the topic (Zhang et al., 2017) and minimal availability of products on the market, with just four among 108 commercially available BIPV products summarised by Frontini et al. (2015), falling in the category of PVSDs. The two aspects are strictly correlated since there would not be any novel product on the market in the short future if the research would not firstly advance. The recent trend is nevertheless encouraging, showing a progressively higher number of researches and papers published each year on the topic as is visible in **Fig. 1**.

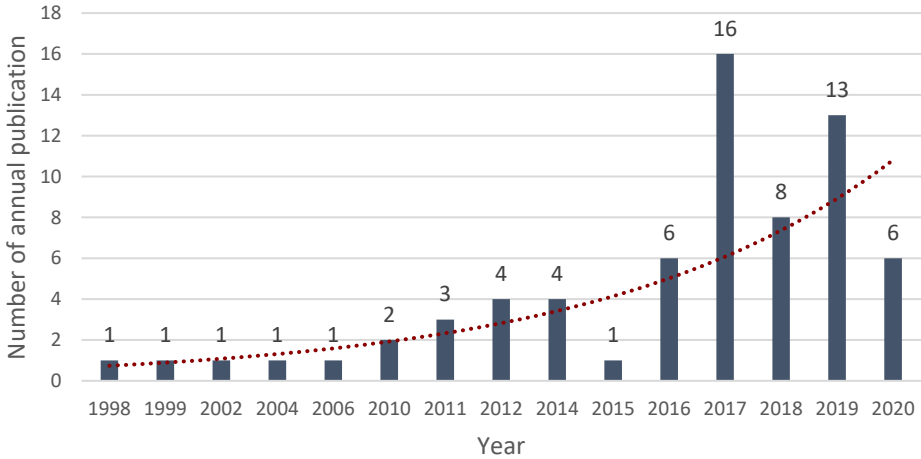


Fig. 1. Chart of publications in the last twenty years with PVSD as topic; image modified from Zhang et al., 2018

1.1 Aim of the thesis

This thesis aims to contribute to broadening the potentialities on photovoltaic shading devices. This is done through the development of a replicable methodology using open-source tools (Grasshopper, Ladybug, Honeybee) to optimise dynamic PVSDs in different latitudes and for different time characterisations in terms of total energy consumption and daylight. Besides that, another goal is to assess if an optimised dynamic shading system performs better than the best available fixed-configuration and to what extent this depends on the frequency of changes in angles along the year. In addition, the fact that different locations situated at different latitudes are compared under identical conditions allows defining a set of general rules which could be used as a starting point for further design approaches.

1.2 Thesis outline

After the introductory **Chapter 1**, the thesis is structured as follow: **Chapter 2** includes a presentation of what BIPV and PVSD are, together with the theory behind the developed method, with a specific focus on daylight simulation. **Chapter 3** defines the research questions, settings and methodology followed to develop the thesis. **Chapter 4** presents the results of the thesis and discusses them together with the limitations of the study. **Chapter 5** is the conclusion, where the main findings are summarised as well as proposals for further developments of the project.

2 Background

In this section, a brief background regarding the technologies taken into consideration is provided, in order to give the reader a better framework of what building-integrated photovoltaics are and why the integration on shading devices is particularly promising. After this first part, the focus is moved on presenting the used tools together with a description of daylight simulation methods encountered and which one has been selected over the others.

2.1 Building Integrated Photovoltaics

According to the definition given by the International Energy Agency, photovoltaic modules can be considered to be integrated into a building when they constitute a construction product providing a function, without compromising the building's integrity (2018). Their first development can be traced back to the end of 70s in the United States, but it is only in the 90s that this technology has started to get more attention (Zhang et al., 2018). Nowadays, they provide a significant contribution to meet the energy reduction goals set by EU countries in compliance with the Paris Agreement.

A great variety of building surfaces can be considered available for the integration of a photovoltaic system, making possible a classification of them into four macro-categories, although a commonly accepted subdivision has not yet been reached (Frontini et al., 2015).

- PV facades: curtain walls, cladding, spandrel panels, balconies, etc.
- PV roofs: tiles, panels, skylights, etc.
- PV windows: glass-glass laminated, transparent thin films, etc.
- PV sunshades: panels, louvres, blinds, etc.

2.1.1 Advantages of Photovoltaic Shading Devices

Among the four categories over exposed, the focus of the current study is on the latter, of which an example is visible in **Fig. 2**. The origin of photovoltaic shading devices is relatively recent, with the first recordable example described by Yoo and Lee (1998), where PV modules were integrated into the roof and south façade of an office building in South Korea. Their use is strictly related to the indoor thermal and visual comfort thanks to the primary role they play as shading devices.



Fig. 2. A PVSD product by the company SolarGaps installed in the World Trade Center office building in Barcelona (Spain) (SolarGaps, 2020)

The advantages of this technology are manifold and can be listed as follow:

- Producing electricity directly on-site through unwanted solar radiation that would be otherwise be reflected away by a conventional system (Bahr, 2014; Zhang, 2014)
- Reducing the cooling load of the building preventing overheating and act as a filter for natural light, improving the visual comfort (T. Hong et al., 2017; Mandalaki et al., 2014)
- Combining two functions, allowing a save in terms of material use, especially for PV assembly components as brackets or rails (Perez et al., 2012)
- Enforcing a specific architecture expression, thanks also to the use of modern photovoltaic materials such as coloured or semi-transparent PV (Hestnes, 1999; Nagy et al., 2016)

2.1.2 Optimal Materials for Photovoltaics Integration in Shading Devices

Regarding the best photovoltaic technology for integration with these devices, the second-generation PVs (thin-film solar cells) have proven to be particularly suitable (Zhang et al., 2018), especially when the integration happens into blinds with a relatively small space between them. Representative of this category are amorphous silicon cells (a-Si), cadmium telluride cells (CdTe) and copper-indium-gallium-selenide cells (CIGS), with the latter offering the highest efficiency among the category. Compared to first-generation products (mono and polycrystalline), thin-film presents a lower conversion rate efficiency (9-14% for CIGS) (Walker, 2013) but they are more tolerant to high temperatures and less influenced in the energy output by partial shading (Bahr, 2014; Dolara et al., 2013; Khaing et al., 2014). Moreover, the lightweight that characterises these products makes them more suitable for being integrated into a shading device (Hong et al., 2016), due to the typically limited bearing capacities of these components.

2.2 Parametric design

The term parametric has its origins from the analytical world, referring to the use of changeable variables and parameters, able to modify the final results of the equation (Frazer, 2016). First notions of the concept applied in the field of architecture and design can be found in the publication of the Italian architect Luigi Moretti, dated back to 1940. In his book *Writings of Architect* (Moretti et al., 2000), he discussed parametric architecture, giving his definition of it as the investigation of architecture systems with the objective of “defining the relationships between the dimensions’ dependent upon various parameters.”

Although the concept has been around for nearly one century, its extensive application to architecture and other associated fields is relatively recent and strictly correlated to the steady development in computational power. The last years have seen the proliferation of software for parametric design, which are getting increasing attention due to their vast potential. These tools can provide architects with the possibility of changing the design of a building or a component, avoiding the recreation of the entire model. The simple modification of sliders or analytical expressions set up in the initial phase of the modelling will result in different geometrical outputs, allowing the investigation of an indefinite number of solutions with substantial timesaving.

2.2.1 Grasshopper: an open source visual language for architects

The best known and appreciated tool for parametric design is Grasshopper, an open-source graphical algorithm editor connected to Rhinoceros 3D, developed by David Rutten and Robert McNeel & Associates starting from 2007. The key to its success is the user-friendly interface, which allows designers without prior programming language skills to use it in a relatively straightforward way. Different components are dragged onto a canvas and connect inputs and outputs through nodes in writing a formula consisting of multiple parameters. The modification of these lasts implies a real-time change of the geometry, visualised in the Rhinoceros environment (Eltaweel and Su, 2017).

2.3 Ladybug tools

Another aspect that makes Grasshopper a valuable tool for the industry and research is the availability of a large number of plug-ins, able to widen its potential. In the development of this study, the Ladybug Tools have been used extensively. This family of plug-ins was started in 2012 to raise the awareness of people on environmental principles in buildings, as well as simplify a fragmented workflow by trying to connect different simulation engines under a single domain. The result is a comprehensive solution for environmental design, which allows a dynamic coupling between the flexible and user-oriented visual programming interface of Grasshopper and popular simulation engines (Ladybug Tools, 2020).

Specifically, the thesis adopted two of these environmental analyses plug-ins for its development. The first is Ladybug, use to import standard EnergyPlus Weather files (.EPW) and generates a wide range of 3D interactive charts, helpful in the initial design stage to support the decision-making process. The second one is Honeybee, able to connect four validated simulation engines (EnergyPlus, Radiance, Daysim, and OpenStudio) and evaluate building energy consumption, daylight, and comfort. (Roudsari, 2013)

The wide range of possibilities offered by Grasshopper and its plug-ins have allowed performing the entire research in the same working environment, avoiding a continuous switch among software usually disconnected with each other and guarantee a higher level of interaction between results. The only process conducted outside the Grasshopper's environment has been the data evaluation, where Microsoft Excel has been used. In the next sections, an excursus on daylight principles and techniques used in the development of the thesis is presented.

2.4 Daylight simulations

As stated earlier, Honeybee uses Radiance and Daysim (an annual daylight simulation software) to run daylight analysis. Radiance first release was in 1989 by the Lawrence Berkeley National Laboratories. (Saxena et al., 2010). The program has seen a constant development and maintenance during the years as well as different validation processes through empirical studies (Grynberg, 1989; Mardaljevic, 2001, 2000, 1995; McNeil et al., 2013; McNeil and Lee, 2013; Reinhart and Walkenhorst, 2001), which makes it one of the most used and appreciated lighting simulation and rendering software on the market.

2.4.1 Light ray-tracing technique as a base for simulations

Radiance is based on the light ray-tracing technique to calculate daylight results. There are two different ways of using this technique, depending on the rays emitted in the scene come from the light source (forward ray tracing) or the test points (backward ray tracing) (Larson and Shakespeare, 1998). The one used by Radiance is the latter, which is faster than its counterpart since it only computes the rays reaching the object of the light (Iversen et al., 2013).

Rays are emitted from the source of interest (usually a grid of points representing the test area) and are traced backwards until they get in contact with a light source (celestial hemisphere or sun) or an object. When a ray hits a surface, a secondary ray is emitted, with an angle and intensity depending on the optical surface's properties (Hensen and Lamberts, 2019). This process is repeated until the ray finds its way to the light source unless a certain number of ambient bounces is reached or if the relative weight of a ray falls under a given threshold value (Larson and Shakespeare, 1998). A representation of this concept can be found in **Fig. 3**.

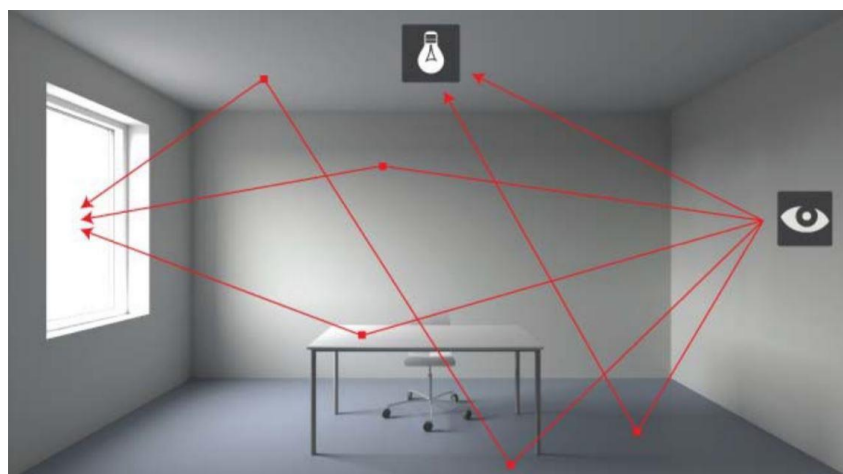
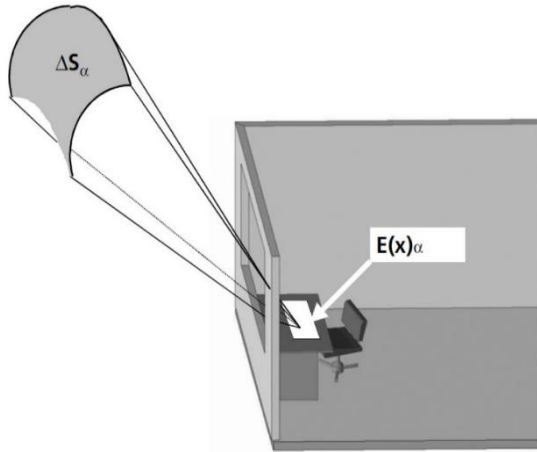


Fig. 3. Representation of the backward raytracing method; image credits: Iversen et al., 2013

2.4.2 The Daylight Coefficients Method

The backward raytracing technique is at the base of every Radiance simulation, including the Daylight Coefficients (DC) method, which is the most used for daylight calculations with standard geometry (**Fig. 4**). The main principle at the base of DC method implies that the incident direct or indirect daylight on a room's surface can be evaluated using the luminance of the sky and the geometry and optical properties of the surrounding surfaces (Subramaniam, 2017). Following this principle, a daylight coefficient can be defined as:



$$[1] \quad DC_{\alpha}(x) = \frac{E_{\alpha}(x)}{L_{\alpha}\Delta S_{\alpha}}$$

where:

x : point and orientation in a building;

S_{α} : sky segment

ΔS_{α} : angular size of S_{α}

$E_{\alpha}(x)$: illuminance at x due to S_{α}

L_{α} : luminance of S_{α}

Fig. 4. Schematic diagram of the Daylight Coefficients Method; image credits: Reinhart, 2001

The inversion of the previous formula makes possible to retrieve the equation for the illuminance at a given point, given by the multiplication between a specific daylight factor and the luminance of the sky segment:

$$[2] \quad E_{\alpha}(x) = DC_{\alpha}(x) \cdot L_{\alpha}\Delta S_{\alpha}$$

The luminance value for the sky is usually coming from Typical Meteorological Year (TMY) weather data (Subramaniam, 2017), available for different geographical locations usually stored inside Energy Plus Weather (EPW) (Subramaniam, 2017). This last formula can be used to retrieve the total illuminance by repeating the calculation for every patch in which the sky is divided and summing up together all the values. Another possible way to express the same formula is by using matrices as:

$$[3] \quad E = C_{dc} \cdot S$$

where C_{dc} is the Daylight Coefficient Matrix, and S is the Sky vector.

2.4.3 Complex fenestration surfaces simulation problems

Despite the standard DC method has proven to be suitable for the vast majority of daylight simulations involving simple glazing and shading systems, when the scene presents complex fenestration surfaces (CFS), its uses alone start to show limitations, becoming inefficient if not completely unreliable (Hensen and Lamberts, 2019). That occurs because is difficult for rays coming from the test points to pass through small and crowded geometrical entities such as the slates of a Venetian blind, causing most of them to remain trapped, giving a lower illuminance value as a result.

A partial solution to the problem consists of sharply increasing specific parameters of the calculation, such as the number of ambient bounces (-ab) and ambient divisions (-ad), raising in this way the chances for the rays to get through the shading device. However, the computational time required for high-resolution settings can take several hours according to the complexity of geometry, making the process inefficient, especially if multiple solutions have to be tested.

2.4.4 Bidirectional Scattering Distribution Functions: a solution for CFS

A valuable option can, in this case, be found in the use of Bidirectional Scattering Distribution Functions (BSDFs). These entities express how the light interacts with a particular material, together with the quantity and direction of transmitted and reflected light. To better understand the meaning of it, a comparison can be made with the lighting design: a BSDF file stays to a fenestration product as an IES file stays to a luminaire (McNeil, 2015).

There are two available possibilities to generate a BSDF file: using the genBSDF tool incorporated in Radiance, which requires a basic knowledge of programming and the ability to use a shell prompt or through the LBNL Window software. The result is a file in XML format, defining light transmittance through the fenestration assembly. More specifically, the light impinging the exterior surface is represented by 145 exterior vectors, a number that comes from the 145 patches in which the program discretises the hemisphere. In the same way, the transmitted light exiting the assembly is described with other 145 interior vectors (**Fig. 5**). Therefore, the BSDF file can be visualised as a collection of coefficients that allocate light from each exterior vector to each interior one.

What is obtained is a 145 x 145 square matrix, where every column represents an exterior vector and every row an interior vector (Saxena et al., 2010). The amount of transmitted light by any interior vector can be described in the formula [4]. In this way, it is possible to model a CFS using a BSDF included in the scene, drastically reducing the computational time of the simulation, and delivering more consistent results.

$$[4] I_j = \sum_{k=1}^{145} c_{jk} E_k$$

where:

I_j : light along the interior vector j

E_k : light along the exterior vector k

c_{jk} : coefficient that relates I_j to E_k stored in the cell located in column k , row j of the BSDF

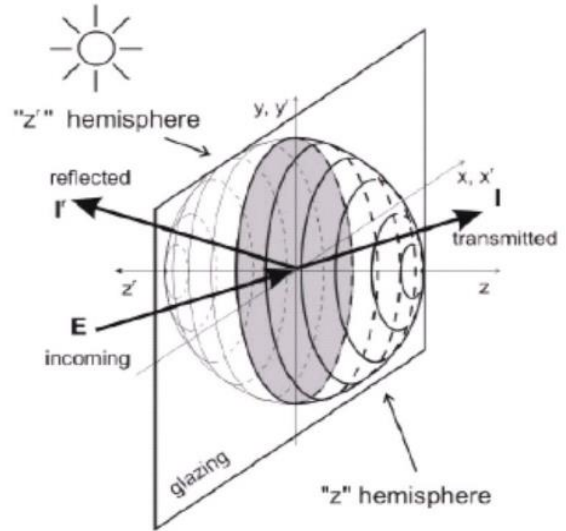


Fig. 5. Representation of interior and exterior vectors of a BSDF; image credits: Fernandes, 2006

2.4.5 Limitations of Daylight Coefficients Method

Despite the opportunities opened by using this approach, there is still a limitation in using it associated to the Daylight Coefficient method. It is, in fact, a common practice when running daylight analysis, to just iteratively evaluate a defined object of the entire scene, while all the rest is kept unchanged. This is especially true when the objective of the study is a dynamic component, as a shading device, able to assume different configurations for different time steps. In this specific situation the DC method, based on addressing the problem in a single step when tracing the rays from the test points to the light source (sky), becomes highly time-consuming (Subramaniam, 2017). The solution is the use of a relatively new approach called Three Phase method.

2.4.6 The Three-Phase Method

The Three-Phase method allows to run annual or point in time daylight simulation for complex and dynamic fenestration systems (McNeil, 2013; Subramaniam, 2017; Saxena et al., 2010). The starting point is the Daylight Coefficient method, but here the flux of transfer path is split into three different independent phases as also illustrated in **Fig. 6**:

1. **View (V)**: flux going from the test points inside of the room to the inner side of the CFS.
2. **Transmission (T)**: flux transmitted through the CFS using a BSDF.
3. **Daylight (D)**: flux from the outer side of the CFS to the sky.

The same concept can also be expressed through multiplications of matrices with the formula:

$$[4] E = VTDS$$

where:

E: matrix containing illuminance results.

V: view matrix, relating incident vectors to the inner side of the CFS.

T: transmission matrix, is the BSDF file that puts incident and exiting vectors in connection.

D: daylight matrix, relating vectors exiting from the CFS to the sky patches.

S: sky matrix, a collection of sky vectors.

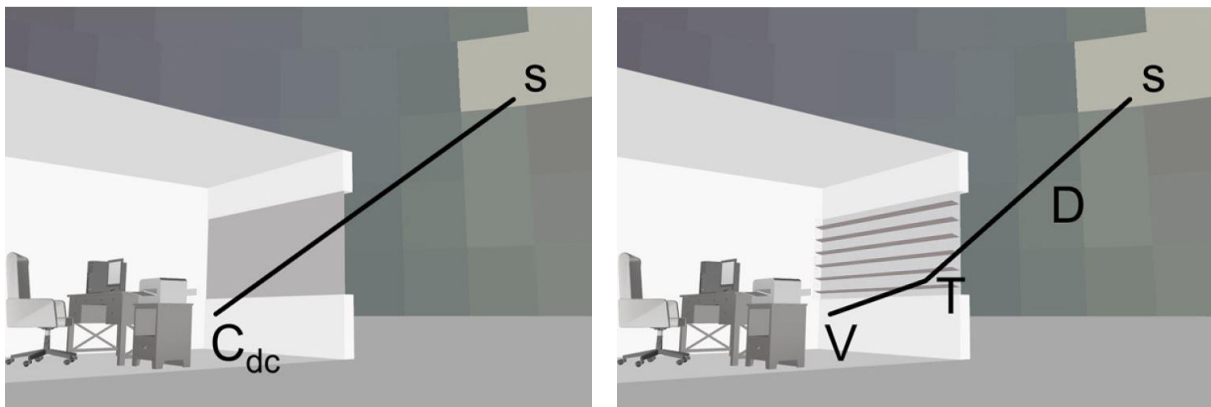


Fig. 6. Comparison between the Daylight Coefficients (left), and the Three-Phase (right) methods; image credits: Subramaniam, 2017

The advantage of using this methodology resides in the chance of experimenting with a large number of configurations for a complex fenestration system in a reasonable amount of time. If there are no changes in the location of the case study and the scene, the calculation of V, D, and S matrices is just executed once and then stored by the program.

The simple modification of the T matrix, correspondent to a BSDF, allowed to investigate different solutions (in our case a range of orientations for a Venetian blind system) by merely multiply the four matrices together.

2.5 A new plug-in for advanced users: Honeybee [+]

Even though the vast possibilities offered by Honeybee, the Legacy plug-in does not support the Three Phase method and neither the use of BSDF. This is consequently to the fact that the program combines of Radiance and Daysim to run annual daylight simulations, inheriting the limitations of this last one. Daysim also has limits regarding the number of window groups and shading states that can process, which makes it unsuitable for simulation with multiple shading control logics or a large number of different configurations (Roudsari, 2018).

In the attempt to overcome these limitations, an evolution of the Legacy plug-in called Honeybee [+] has been under development for several years. Although it is not yet covering all the aspects (energy simulations are not available yet), it is entirely usable for daylighting. Here Daysim is replaced totally by Radiance, taking advantage of the new calculation methodologies implemented in the meanwhile together with the possibility of using BSDFs to discretise complex fenestration surfaces.

The decision tree in **Fig. 7** helps to understand which method of simulation to choose according to the type of system and conditions that have to be tested. In the case of the current study, since the simulation is supposed to be run for an entire year, the solution is a dynamic sky.

Regarding the second step, the geometry does not present any changes in the context and neither in the interior, but the dynamic nature of blinds does not permit to go for a Two-Phase simulation (another name to call the DC method since the calculation is solved in two passages). The presence of multiple glazing does not present an issue since the windows of the case study present the same control logic and can, therefore, be put in the same Window_Group.

The Six and Four-Phase methods are not implemented in Honeybee [+] leaving open the choice between the Three and the Five-Phase methods. Being the focus of this thesis not on the effect of direct daylight since glare is not considered among the optimisation parameters, a lower spatial resolution with the use of the Three-Phase method was judge adequate to the final objective.

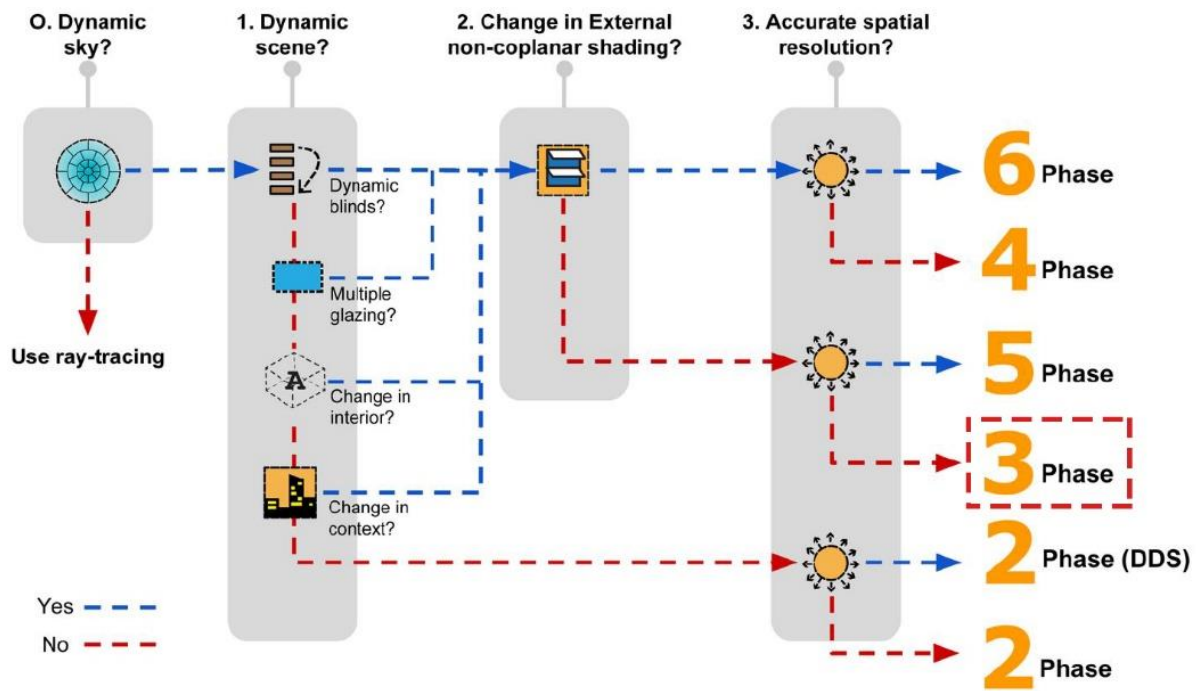


Fig. 7. Simple decision tree to select the best simulation according to geometry and objectives of the study; image credits: Mostapha Sadeghipour Roudsari

3 Methodology

The methodology used in the study stems from the one proposed for the first time by Taveres-Cachat et. Al. (2019). That specific publication was also used to identify the optimal number of louvres to use as a starting point and primary object of comparison for different locations, since was proved that, for a fixed PVSD located in Oslo, the best number of louvres is 16. The dynamic nature of the current study has required an adaptation of the existing methodology, with the addition and modification of several steps. The main changes occurred for the daylight calculation, where the Three-Phase method, able to support the dynamic behaviour of the blinds, was chosen. An exhaustive description of the reason why that specific technique was used over others is presented in the background.

In the following sections, a description of settings and the method adopted throughout the research is provided, while the next two pages show a flowchart summary of the methodology (**Fig. 8**) and the workflow developed in the Grasshopper environment (**Fig. 9**).

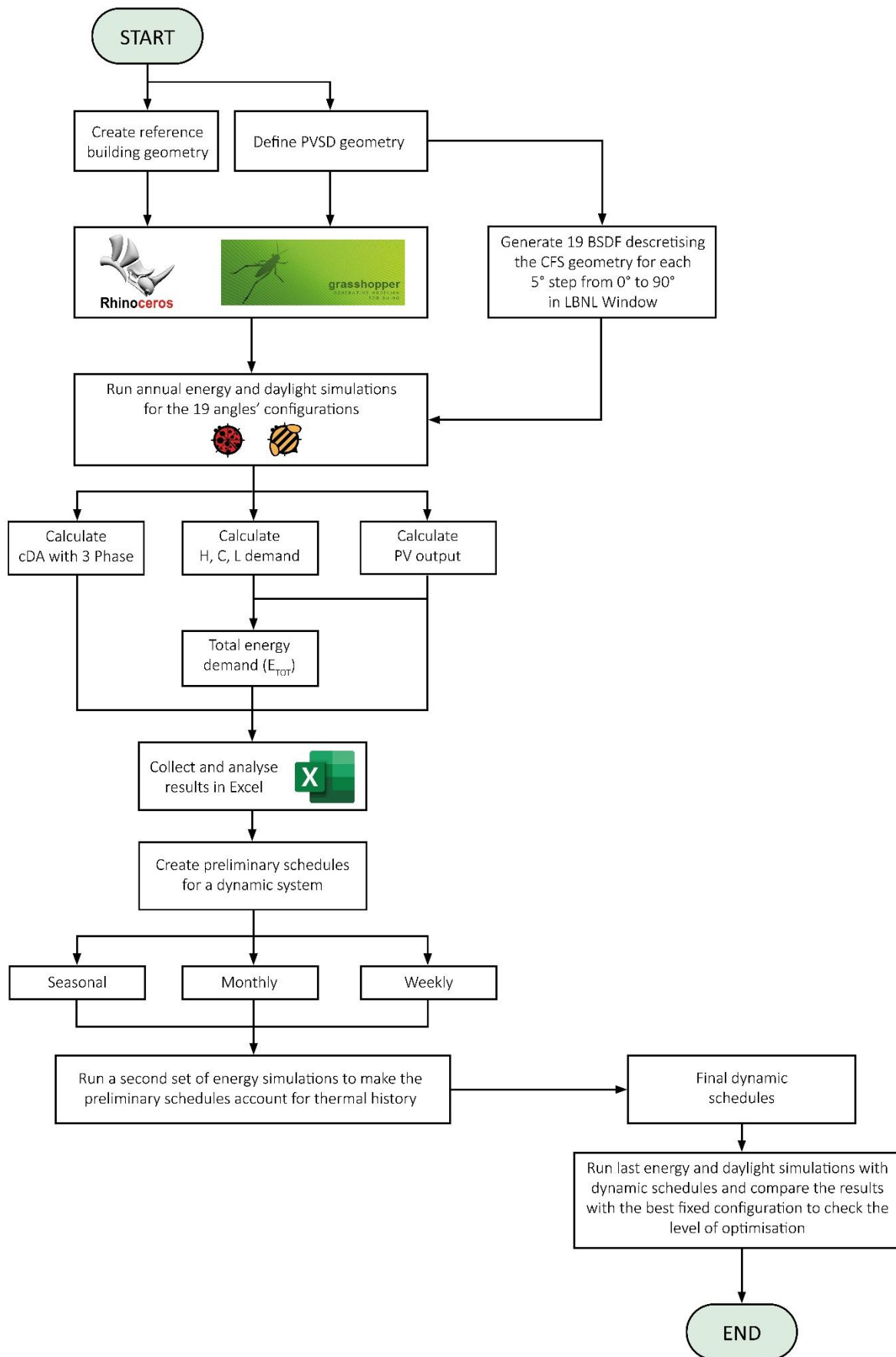


Fig. 8. Flowchart summary of the design methodology

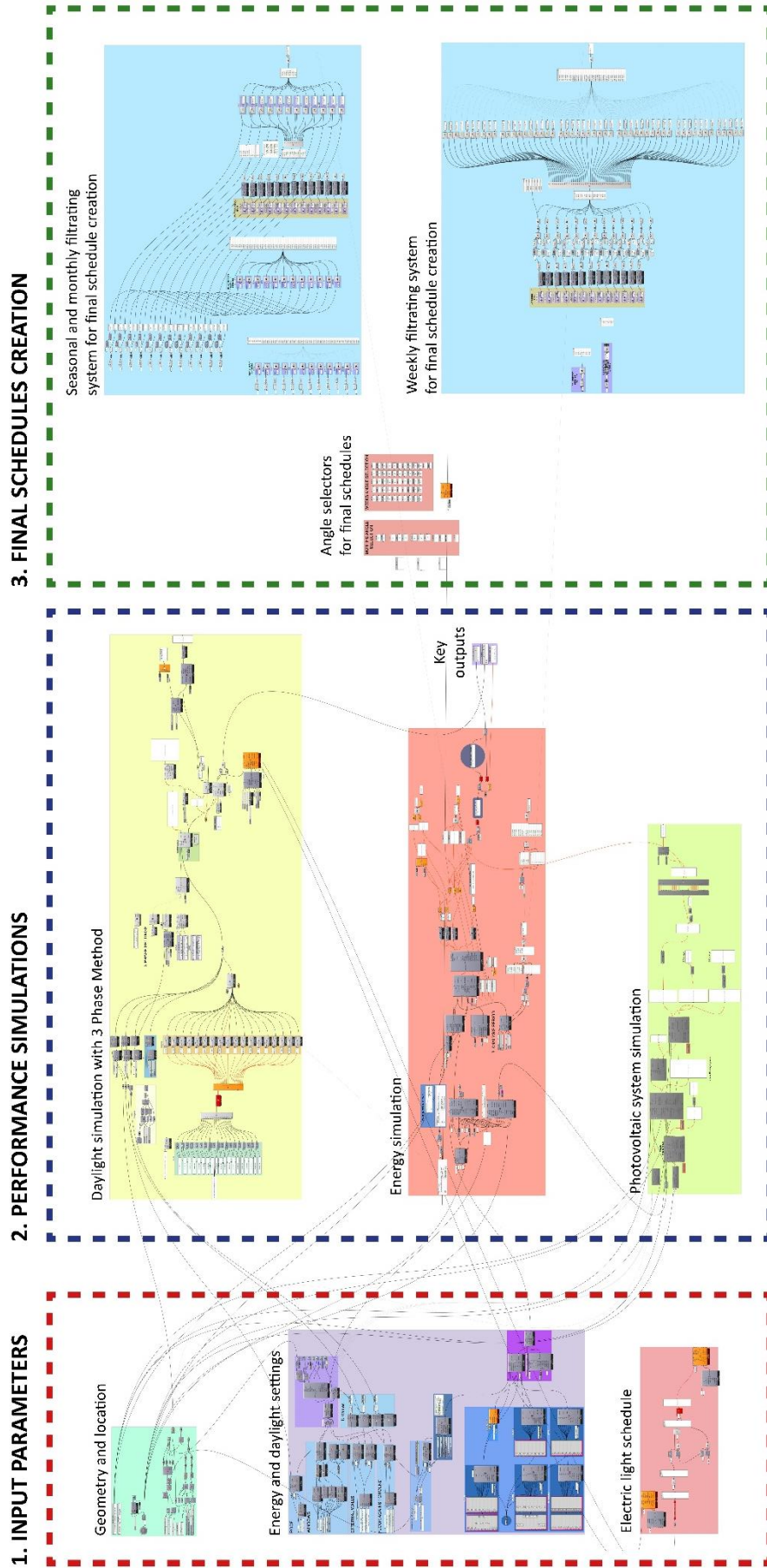


Fig. 9. Visualisation of the workflow developed in the Grasshopper environment

3.1 Geometry Description

The case study was modelled entirely parametrically in Grasshopper environment, keeping open the chance to modify dimensions freely. The tested geometry (**Fig. 10**) is the Bestest Case 600, a 48 m² facility with a rectangular shape (6 m × 8 m × 2.7 m) and two south-facing windows (3 m × 2 m). The photovoltaic shading device system has a slat width of 105 mm and a spacing between elements automatically generated according to the number of louvres. The standard configuration used in the study as a reference case has 16 louvres, spaced of 125 mm. The PVSD system is located in front of both windows at 20 cm from the exterior pane, while the louvres are free to move from 0° to 90°, with an increment of 5°.



Fig. 10. Views of the geometry of the Bestest Case 600 in Rhinoceros 3D environment

3.2 PV Settings

As described in the background, good options for the integration of PV into shading devices were proven to be the thin-film technology as the CIGS and a-Si cells (Hong et al., 2016; Jeong et al., 2017). For this study, GIGS cells have been chosen, with the photovoltaic material imagined covering the 95% of the upper side area of each blade of the shading device.

The conversion efficiency is set to 15%, and the value taken as energy production is the alternate current. Considering that is not possible to account for the loss in production caused by the self-shading of the system by merely using the standard PV calculator component present in Ladybug, the simulation for PV production was run twice, adding the second time a derate factor. This value is the result of an accurate shadow analysis of the blinds' geometry, which calculates the amount of solar radiation that is effectively falling of the PV surfaces for the current configuration. With this approach, it is possible to get a more reliable value for the energy production, despite the need of running three simulations in series (PV simulation – shadow analysis – PV simulation with derate factor).

This procedure is relatively time-consuming (around 8 minutes for each configuration) and was judged inefficient to repeat it cyclically in searching of the optimal solution among the 19 different angle configurations that the dynamic system can potentially assume. To address this problem, for every studied location, a series of simulations were firstly run for every 5° step. The results, consisting of lists of 8760 hourly values, were stored into specific Grasshopper components, ready to be filtrated in a second phase accordingly to the required time step (seasonal, monthly, or weekly).

3.3 Energy settings

In the set-up of the energy model, the Norwegian Standards NS 3031:2016 and NS3701:2012 were used to define internal loads and schedules for office building category. In **Table 1**, the building envelope's properties and technical system are listed.

Table 1. Thermal properties of the envelope and technical systems; adapted from Taveres-Cachat et al., 2019

COMPONENT	VALUE	UNIT
U - value external wall	0.18	W/(m ² K)
U - value roof	0.13	W/(m ² K)
U - value floor against the ground	0.1	W/(m ² K)
U value window (3 panes)	0.8	W/(m ² K)
Airtightness	0.6	h - 1
HVAC system	Ideal air load	-
Internal load lighting	9.6	W/m ²
Maximum internal load occupants	382	W
Maximum internal load equipment	21	W/m ²
COP heating	3	-
COP cooling	5	-
Setpoints (heating-cooling)	20-24	°C
Occupation hours	7, 18	-

When writing a definition for a simulation, a series of components are logically connected. A component can be defined as an entity that encapsulates a range of selectable options on one specific theme. Usually, these options are the same available inside the simulation engines (EnergyPlus, Radiance, Daysim, or OpenStudio), which run in the background during the calculation process. The substantial difference in using a visual programming approach as in Grasshopper, is the availability of options always-on display and the easiness of selection, compared to the need of choosing from extensive lists of submenus in the native software.

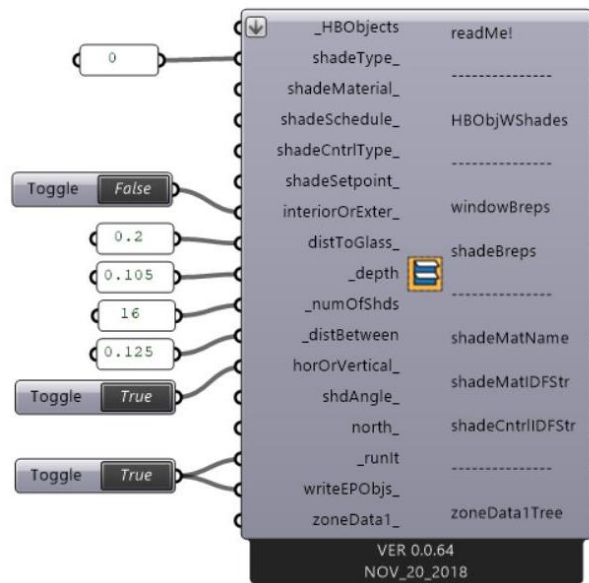


Fig. 11. Honeybee_EnergyPlus Window Shade Generator component

In **Fig. 11** is visible one of the important components used in writing the definition of the energy simulation, which allows the generation of a shading device, starting from the geometry of windows as input. Several inputs are available to be selected on the left side of the component, as the shading type, its orientation and position, dimension, number and spacing of louvres. For the study, the PVSD is imagined to be always lowered down in front of the window, free to dynamically adjust the angle of all the louvres simultaneously for different time steps, according to a predefined schedule.

The component has an option to input a schedule, controlling if the shading system has to be lowered or raised (`shadeSchedule_`) but is apparently missing the possibility of changing the tilt angle of the louvres in the same way. It was found that the developers consciously decided not to insert this feature, even if it is present in EnergyPlus, in order not to make the component too large and complex. Nevertheless, they inserted the option in the coding strings, as visible in **Fig. 12**, leaving the user to manually edit the script if needed. By changing line 1123 of the script from `FixedSlatAngle` to `ScheduledSlatAngle` and inserting in line 1127 the schedule's name, it was possible to control the inclination of the blinds according to a schedule, making in this way the system dynamic along one year period. The next and final step has been to write additional strings using the correct syntax and connect them to the component in charge of running the energy simulation (Honeybee_Run Energy Plus) to provide the program with the right path on the machine where to find the control schedule for the dynamic system.

An attempt, using shading fractions to discretise the CFS geometry and create a transparency schedule able to simulate the effect of dynamic louvres was tried before adopting the Three-Phase method. However, it was proven that the component in charge of generating the transparency schedule only works for the energy part, while it does not affect daylight simulations, which ultimately clarifies the right approach to follow.

In the configuration of the Three-Phase method a Window_Group, including both the south-facing windows sharing the same logic, was created. Nineteen states, describing the geometry of louvres for each 5° step from 0° to 90° in the form of BSDFs .xml files, are connected to the window group. The .xml files were generated using the LBNL Window 7.7 software, where the glass layers were created, together with the shading device in front of them (**Table 3**) (Mitchel et al., 2019). The total visible transmittance (T_{vis}) for the triple-pane glass is 0.60, while the total visible reflectance (R_{vis}) is 0.2. Although the louvres' material is aluminium, which usually has a R_{vis} of 0.65, a value of 0.13 was set due to the CIGS cells coating layer, that has a much lower reflectivity index.

Table 3. Layers composing the complex fenestration system; T_{sol} : solar transmittance, R_{sol1} : solar reflectance exterior facing side, R_{sol2} : solar reflectance interior facing side, T_{vis} : visible transmittance, R_{vis1} : visible reflectance exterior facing side, R_{vis2} : visible reflectance interior facing side

LAYERS	NAME	THICK (mm)	T_{sol}	R_{sol1}	R_{sol2}	T_{vis}	R_{vis1}	R_{vis2}
OUTSIDE								
Shade 1	Venetian blind	105.0	0.001	0.234	0.234	0.0	0.133	0.133
Gap 1	Air	200.0						
Glass 1	Ultra clear glass	4.6	0.902	0.082	0.082	0.911	0.085	0.085
Gap 2	Air (10%) /Argon (90%) Mix	16.0						
Glass 2	Low E-coating glass	5.0	0.497	0.334	0.234	0.801	0.801	0.112
Gap 3	Air (10%) /Argon (90%) Mix	16.0						
Glass 3	Low E-coating glass	5.0	0.497	0.334	0.234	0.801	0.801	0.112
INSIDE								

The analysis grid on the tested geometry has a size of 1 meter, resulting in 48 test points, and is located at 0.8 metres from the floor to simulate the high of a working plan. The sky used for the annual daylight simulation is based on the Tregenza sky model that is divided into 145 sky patches. The Radiance settings for the simulation are visible in **Table 4**. Two different lists of settings (low and high) were tested in order to conduct a sensitivity analysis on how higher parameters can influence the accuracy. However, the results have shown a difference lower than 2% between the two cases, while the computational time passes from 13 to 47 minutes.

These findings have determined the adoption of low settings for the simulations. The small difference is related to the fact that in the Three-Phase analysis these settings influence just the V and D Matrices, while the T Matrix representing the most computationally demanding part of the simulation (namely the CFS constituted by the shading device and the window) has already been calculated in LBNL Window with the use of BSDFs. The simulations were conducted on a machine with 16 GB RAM, 2.20 GHz processor, and 12 CPU.

Table 4. Radiance settings for the daylight simulation, the lower option was chosen; -ab: ambient bounces, -ad: ambient divisions, -as: ambient sampling, -aa: ambient accuracy, -ar: ambient resolution

	(-ab)	(-ad)	(-as)	(-aa)	(-ar)	TIME (minutes)
LOW SETTINGS	3	1000	128	0.25	16	13
HIGH SETTINGS	5	8000	128	0.25	256	47

3.5 Electric light settings

A schedule for electric light, able to modify itself according to the illuminance level given at a sensor point in the middle of the room, has been created. The aim is to proportionally respond through the dimming of the luminous flux to the variation of natural illuminance, by ensuring a minimum level of 500 lx on a 0.8 meter working plane during the occupational hours. A minimum flux, corresponding to 20% of the total, is always provided, even when the illuminance level is over 500 lx. In **Fig. 13** the annual illuminance registered at the sensor for Oslo with a fixed 16 louvres system at 0° is presented, together with the electric light schedule generated accordingly.

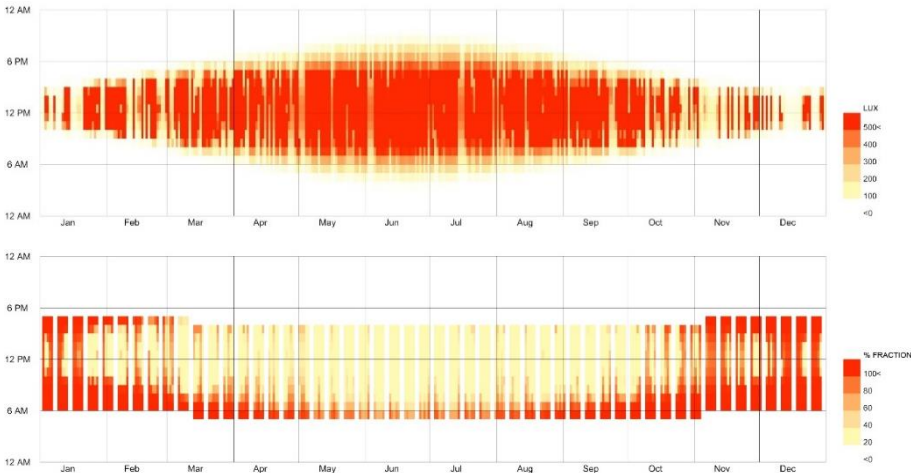


Fig. 13. Diagram of the total illuminance recorded at the test point for one year in Oslo with a 16 louvres system at 0° (upper image) and the electric light schedule which compensates proportionally and keeps the overall daylight value over 500 lux

3.6 Objectives functions of the optimisation

The two objectives functions to be optimised in the simulations were the minimisation of the total annual net energy use E_{TOT} (kWh/m² year) and the maximisation of the daylight level, measured as continuous daylight autonomy (cDA [%]). The total annual energy use E_{TOT} is the sum of electric energy used for heating, cooling, and artificial lighting, plus the electricity produced by the photovoltaic cells integrated into the shading device.

The cDA is a relatively new dynamic daylight metric, proposed by Zach Rogers (2006) from the modification of Daylight Autonomy DA. It is defined as the percentage of annual occupancy hours during which a specific point in time is above a certain illumination threshold. Differently from the DA, partial credits are also linearly awarded to values below the user-defined threshold (500 lux in this study). The transition between compliance and noncompliance values is in this way softened, and a better picture of the illuminance situation is given (Daylighting Pattern Guide, 2020; Reinhart et al., 2006).

3.7 Selected geographical locations

The study was conducted on four cities located at latitudes ranging from 60° to 30°. This choice was dictated by the will of comparing the effectiveness of a dynamic PVSD under different climatic conditions and levels of solar radiation. Different numbers of louvres have also been tested, introducing in this way a new variable to the study. Despite that, the main focus has been kept on the 16 louvres configuration, which is the only one tested for all the locations, in order to have a precise mean of comparison between considerably different climatic patterns.

The selected cities for the study have been:

1. **Oslo**, located at a latitude of 60° and representative of the Scandinavian area. The Oslo area falls under the category of warm-summer humid continental climate according to the Köppen-Geiger classification. Its high latitude is reflected in remarkable differences in daylight availability along the year, with long days in summer and dark winter.
2. **Brussels**, at a latitude of 50° and characterised by a temperate-oceanic (Cfb) climate. The capital of Belgium is representative of the continental Europe area and is characterised by high levels of sky coverage by clouds (over 50%).

3. **Rome**, located in the middle of the Italian peninsula at a latitude of approximately 40°, is a valuable choice to evaluate the Mediterranean climate (Csa), characterised by dry summers and wet winters.
4. **Cairo**, situated in North Africa facing the Mediterranean Sea at a latitude of 30°; it represents the most extreme choice in terms of weather conditions with a hot desert climate (BWh) and high average temperature all the year.

Only for Oslo, an additional set of simulations, changing the condition for the external surfaces from exterior to adiabatic, was also executed. This test was conducted to understand the difference in results when the simulated volume is imagined to be surrounded by other similar units mimic, for instance, a single office inside of a large office building, and to estimate if a higher contribution of the thermal history is visible in this case. A summary of the information just exposed is visible in **Table 5**.

Although simulations have been conducted for all the position that the dynamic system can assume (19 configurations from 0° to 90° every 5° step), during the optimisation process no angle over 70° have been selected. Therefore, was decided not to include these values in the graphs to provide a clearer lecture of the other data.

Table 5. Overview of the four analysed locations with the number of louvres tested; in red is underline the 16 louvres configuration, which was the main focus of the study *for this specific location and configuration a series of simulations with adiabatic surfaces were also tested

LOCATION	LATITUDE	AVERAGE ANNUAL TEMP.	KOPPEN CLIMATE	TESTED LOUVRES		
OSLO	59.9	6.3°	Dfb (humid continental)	16*	13	10
BRUSSELS	50.5	10.3°	Cfb (temperate-oceanic)	16		
ROME	41.9	15.7°	Csa (mediterranean)	16	13	10
CAIRO	30	21.3°	BWh (desert)	19	16	

Was calculated that during the entire study, almost nine million data have been processed. A brief explanation of how this number was reached is visible in **Fig. 14**.

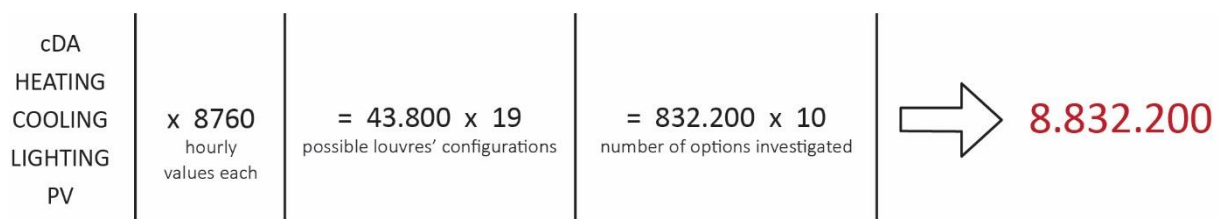


Fig. 14. Summary of the data processed throughout the simulation

3.8 Multi-objective optimisation process

The objectives of the optimisation are competing with each other. High illuminance levels imply the blinds to be fully opened at 0° , while the PV generation and the potential cooling effect offered by the shading device tends to be achieved with higher angles' configuration. A satisfactory balance between them was a primary concern of the methodology in order to reach better overall performance in terms of energy consumption and visual comfort.

That was possible using a logic for the selection of the best angle for the PVSD at each time step (seasonal, monthly, and weekly). It was given attention to the visual comfort by setting the following criteria: when the cDA scored over 50%, the angle which provides the lower E_{TOT} is selected, while when the cDA is lower than 50%, the angle providing the highest cDA is taken, disregarding the E_{TOT} . This selection is operated in Microsoft Excel, where the hourly annual data for heating, cooling, lighting, PV production, and cDA have been processed. The data represent the first set of simulations for the 19 possible configurations that the system can adopt by changing the louvres' angle from 0° to 90° for one of the specific geographical locations objects of the study.

The result of the selection is a preliminary schedule of 8760 values, representing the angles to be applied to the shading device throughout the year. Three schedules with different time characterisations (seasonal, monthly, and weekly) are created for each selected location. This means that for a seasonal schedule, 4 angles alternate themselves throughout the year, for a monthly schedule 12 angles and a for a weekly schedule 52.

Nevertheless, the so-created schedules are not yet the definitive ones; that is because of the role played by the thermal history in the energy calculation. It is essential to remember that the processed values are coming from simulations where, for an entire year, the angle of the PVSD is fixed. It means that when during the selection process an angle is chosen for a specific time step, its E_{TOT} value is misleading, since it is considering that all the previous data comes from a solution where the angles along the entire year are the same.

In order to correctly consider the effect of thermal history, a schedule has to be built up in Honeybee, starting from the preliminary one, through a step-by-step method. Using the monthly schedule as an example, the procedure for its creation is the following:

1. A first simulation is run for the only month of January with the best angle according to the preliminary schedule (the first month is not influenced by thermal history)
2. The analysis period of the simulation is changed, to include February
3. A series of simulations for all the angles that satisfy the $cDA > 50\%$ logic in the preliminary schedule are performed, with January and February as analysis period
4. The best new angle for February is chosen, being this time sure that the correct contribution from thermal history has been accounted
5. The analysis period is modified to include March, and a new series of simulations are run to get the best angle for the new month
6. The process is repeated for all the 12 months, and a definitive schedule is generated

Despite its incompleteness due to the inaccurate thermal part, the preliminary schedule allows for a first screening of the 19 angles' configurations at every time step. When cDA values are lower than 50%, just the 0° option needs to be run for that specific time step in the second round of simulations defining the final schedule. In addition, evidences in processing the results have shown that most of the time the angle selected in the preliminary schedule for a specific time step is already the optimal one and is never out of a range of $\pm 10^\circ$ to the optimum.

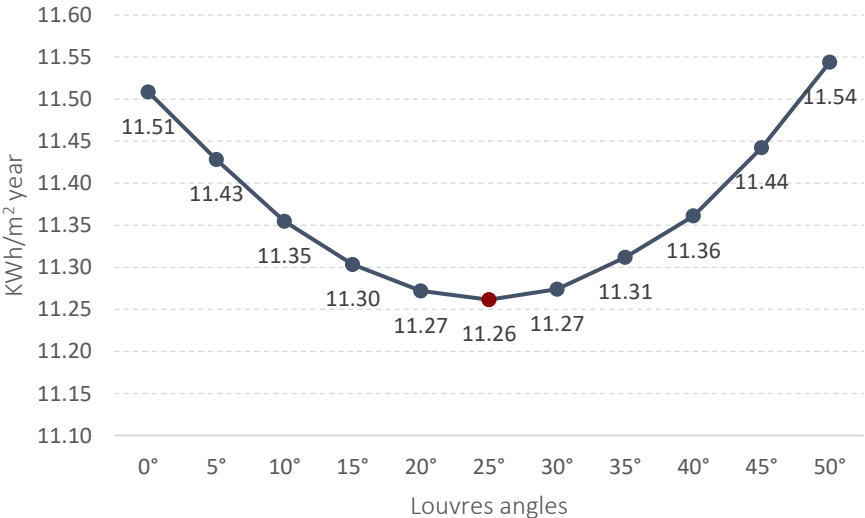


Fig. 15. Chart representing the quadratic trend of the E_{TOT} of the month of July in Oslo for a configuration with 16 louvres; in red is highlight the lower value picked, which correspond at the vertex of the parabola

This can be explained by the fact that when testing different angle options according to the $cDA > 50\%$ logic, the E_{TOT} distribution is always described by a quadratic function, where the lower value is the vertex of the parabola, as is visible in **Fig. 15**. This allowed testing only the angles close to the one suggested in the preliminary schedule (two before and two after), in order to reduce the number of simulations. In **Fig. 16** the process for the creation of a definitive monthly schedule for Oslo with a 16 louvres system is illustrated.

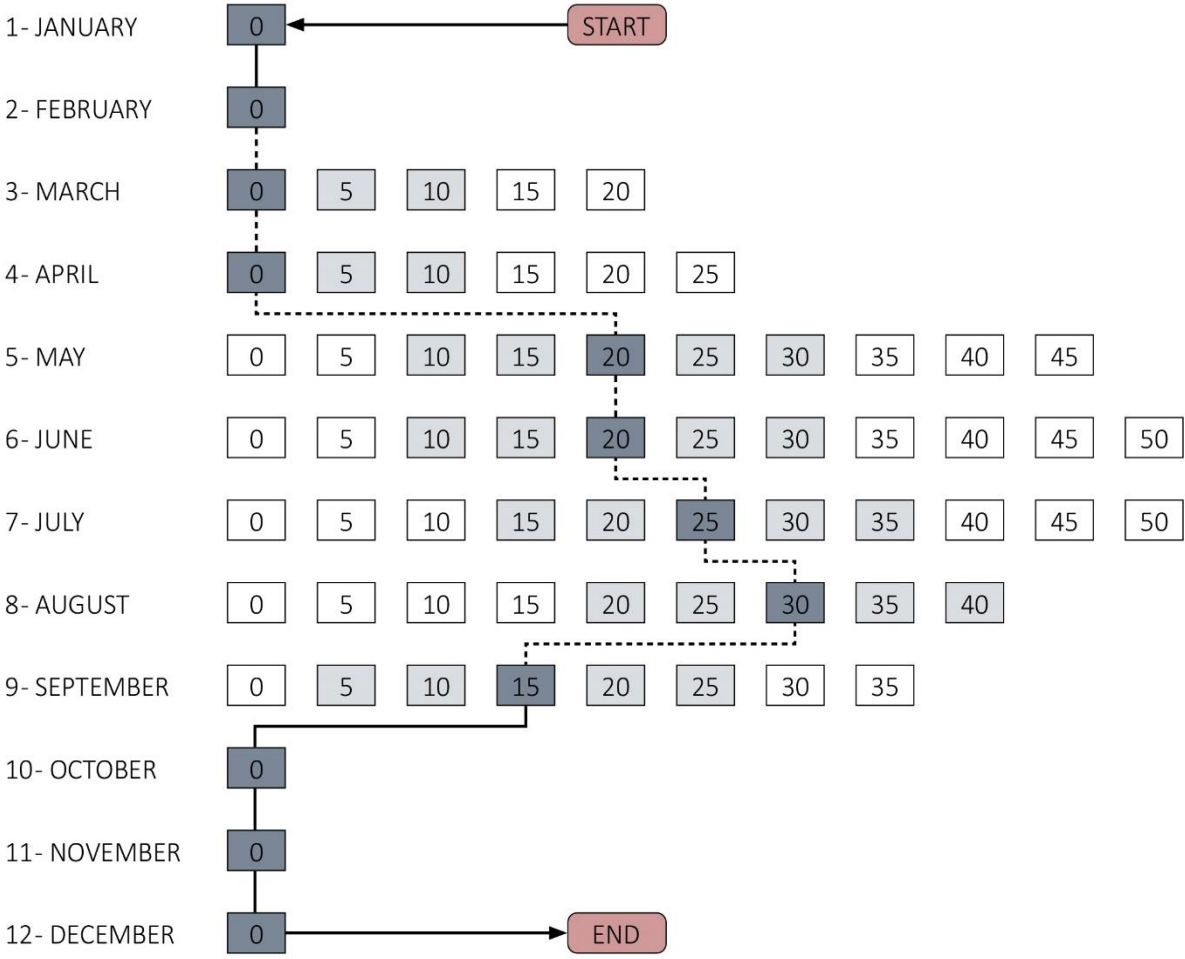


Fig. 16. Diagram showing the passages for the creation of a definitive monthly schedule for Oslo with a configuration of 16 louvres. The boxes with numbers represent the angles to test for every month since they guarantee a cDA level above 50%; the darker blue indicates the best configuration according to the preliminary analysis while the light blue the shows the simulations actually run, taking in consideration the quadratic distribution of the E_{TOT} results

4 Results and discussion

In the following pages, the results are critically discussed and compared to each other. It is essential to underline that the level of optimisation for cDA and E_{TOT} for every location and louvres' configuration, is always obtained by comparing the final results of the dynamic simulation to the best fixed annual configuration for the considered solution.

4.1 Oslo

The first considered location for the study has been the city of Oslo. Trends in the results are visible by looking at the chart in **Fig. 17**, where annual E_{TOT} and cDA for fixed shading systems are compared from 0° to 70° . Minimal levels of electricity for cooling are required, while the significant share of energy is used by space heating. By progressively closing the shading system, heating and artificial lighting demands increase, while the cooling remains almost stable with a small decrease. Regarding PV production, there is a constant increment until the reach of the optimal angle of 40° .

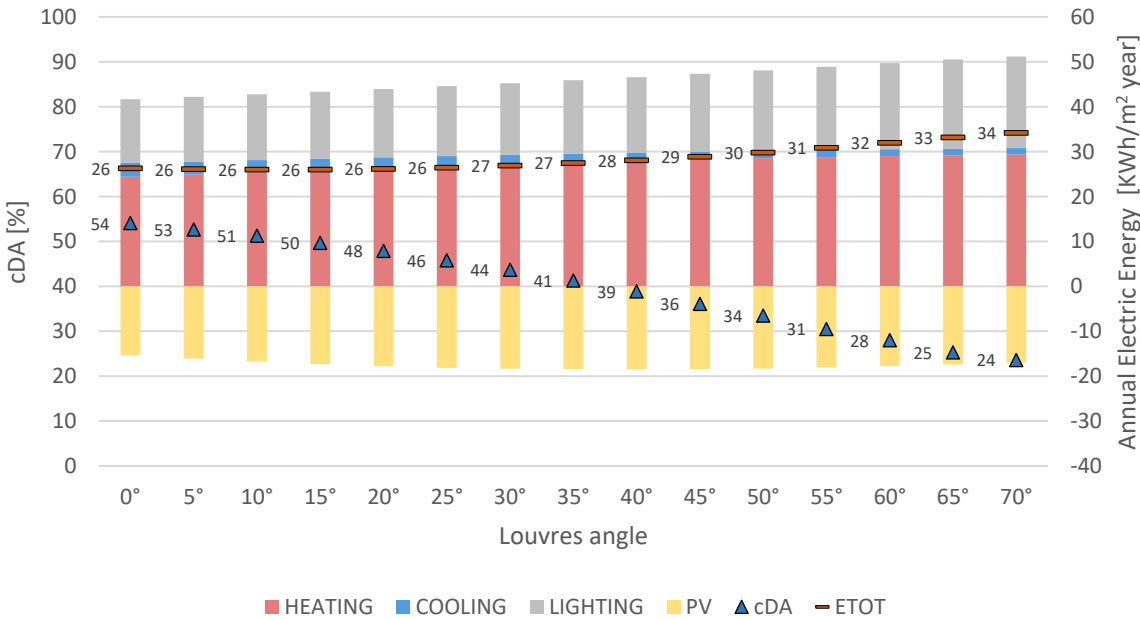


Fig. 17. Chart showing the Oslo 16 louvres share of energy and cDA for the different configurations of the photovoltaics shading device

Higher differences are noticeable in cDA where, already after the 15° , a level outside the acceptable range is reached, making the rest of the configuration unsuitable to be considered given the selected criteria ($cDA > 50\%$).

The best overall configuration here is the one with an inclination of 10°. This first outcome has been used as the reference parameter when creating a dynamic schedule for the shading device. The increment of efficiency in adopting the dynamic solution is calculated in comparison to the best configuration available using a fixed system. The optimisation is executed for three different annual sets, with progressively shorter time steps. This fact implies a broader alternation of angles as the schedule becomes more accurate in following the climatic variations, as is possible to see in **Fig. 18**.

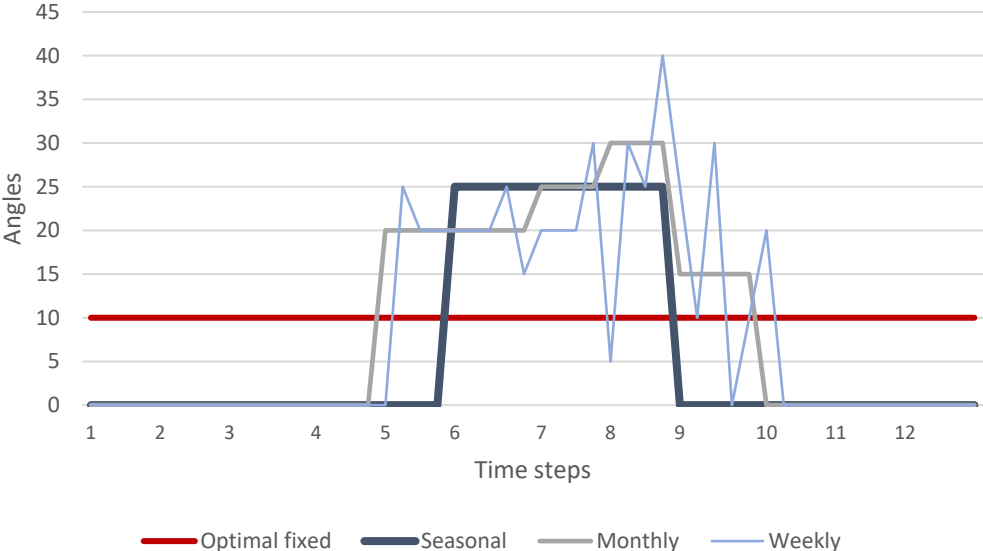


Fig. 18. Chart illustrating angles' alternation for seasonal, monthly, and weekly schedules for Oslo 16 louvres

The optimisation process can be interpreted as a trade-off between daylight and energy consumption, permitting the selection of lower E_{TOT} value at the expense of a fraction of cDA. Therefore, the results present always a lower overall energy consumption with usually a lower daylight value, yet over the accepted threshold of 50%. For the 16 louvres configuration in Oslo, despite an optimisation is reached, the scope of it is limited (**Table 6**). A reason for it is the cold climate that characterises the site, fact that limits the utility of the system in cooling down the building through extra shadows, as well as the scarcer amount of solar radiation collectable by PV, compared to lower latitudes.

Table 6. Overview of the optimisation of a dynamic system over a static one for Oslo 16 louvres

TIME-STEPS	cDA [%]	E_{TOT} [KWh/m ² year]	OPTIMISATION cDA	OPTIMISATION E_{TOT}
FIX 10°	51.3%	26.0		
SEASONAL	51.4%	25.4	0.2%	2.1%
MONTHLY	50.2%	25.2	-2.1%	2.9%
WEEKLY	50.7%	25.1	-1.2%	3.5%

4.1.1 Oslo Adiabatic

The same configuration with 16 louvres has also been tested by changing the condition for the external surfaces from exterior to adiabatic. The E_{TOT} is here drastically reduced and, despite the difference is still contained, adiabatic settings show a greater influence of the thermal history, more visible at shorter time steps (monthly and weekly), where the increment is of almost four times as visible in **Table 7**.

Table 7. Influence of thermal history when the settings of the exterior surfaces are changed from facing the exterior to adiabatic

	TIME-STEPS	E_{TOT} PRELIMINARY SCHEDULE	E_{TOT} FINAL SCHEDULE	% DIFFERENCE
EXTERIOR	SEASONAL	25.5	25.4	0.2%
	MONTHLY	25.2	25.2	0.1%
	WEEKLY	25.0	25.1	0.3%
ADIABATIC	SEASONAL	9.5	9.5	0.2%
	MONTHLY	9.0	9.0	0.5%
	WEEKLY	8.6	8.7	1.0%

Regarding the level of optimisation that is possible to obtain, the adiabatic option shows a high margin of improvement for the energy while the cDA suffers the optimisation consistently. The final values are in fact under the threshold of 50%, deriving from picked values of cDA on average lower when composing the final schedule, even if meeting the $cDA > 50\%$ logic. An additional reflection regarding the adoption of a dynamic system in this particular case should be done since values lower than 50% for cDA are usually not considered optimal. However, these values are just under the acceptability threshold while the optimisation in terms of energy consumption is relevant, especially for the monthly and weekly time steps, as visible in **Table 8**. Would probably be, therefore, beneficial to adopt a dynamic system over a static one also in this specific situation.

Table 8. Overview of the optimisation of a dynamic system over a static one for Oslo 16 louvres adiabatic

TIME-STEPS	cDA [%]	E_{TOT} [KWh/m ² year]	OPTIMISED cDA	OPTIMISED E_{TOT}
FIX 10°	51.3%	9.8		
SEASONAL	49.2%	9.5	-4.1%	2.9%
MONTHLY	48.5%	9.0	-5.5%	8.2%
WEEKLY	48.8%	8.7	-4.9%	11.3%

4.1.2 Oslo 13 and 10 louvres

In order to understand if better results could have been obtained by modifying the number of louvres, solutions with 13 and 10 elements have been tested for seasonal and monthly time-steps. A lower number of louvres in the PVSD results in more space between them, allowing a higher fraction of natural daylight to penetrate the room and consequently reducing the electricity consumption for artificial light. The optimal inclinations for fixed systems are here respectively 15° and 30° for the 13 and 16 solutions, thanks to the broader range of selectable angles without compromising the interior daylight.

Table 9. Overview of the optimised results for 13 and 10 louvres configurations in Oslo and the percentage difference to the 16 louvres configuration for cDA and E_{tot}

	TIME-STEPS	cDA [%]	E_{TOT} [KWh/m ² year]	Δ cDA 16 LOUVRES	Δ E_{TOT} 16 LOUVRES	OPTIMISED cDA	OPTIMISED E_{TOT}
13 BLINDS	FIX 15°	52.4%	27.3				
	SEASONAL	52.7%	26.8	2.5%	5.1%	0.6%	1.8%
	MONTHLY	51.5%	26.4	2.5%	4.6%	-1.7%	3.1%
10 BLINDS	FIX 30°	52.6%	28.9				
	SEASONAL	54.4%	28.7	5.5%	11.6%	3.4%	0.8%
	MONTHLY	53.8%	28.3	6.7%	11.0%	2.3%	2.1%

The results in **Table 9** show an overall higher cDA for both options. However, the E_{TOT} presents slightly larger values than the 16 louvres solution. This is mainly due to the significant impact played by the sharp reduction of PV area, as illustrated in **Fig. 19**, causing an energy production drop of around 12% when having 13 louvres, and almost 27% for 10 louvres. The reduction of self-shading is therefore not compensated for the loss of available PV surfaces, leading to an overall worst result. Further consideration could be made if the energy embedded in the production of the component would have considered: a system with fewer louvres would have, in fact, lower related emissions for its production that could result in a better option.

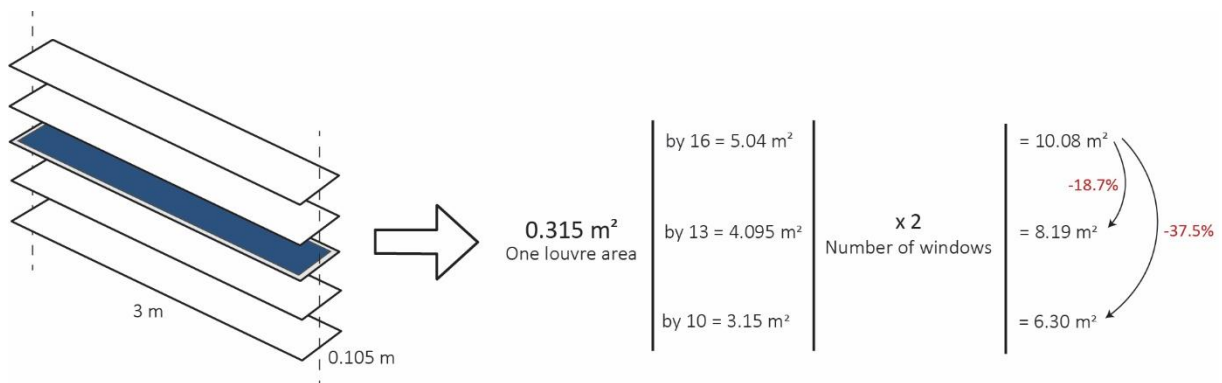


Fig. 19. Illustration showing the reduction in PV area by diminishing the number of louvres

4.2 Brussels

In Brussels, only the configuration with 16 louvres has been tested for the creation of optimised seasonal, monthly, and weekly schedules. Although a slightly higher contribution from PV production would have been expected, the cDA levels are almost equal to the ones measurable in Oslo. This factor can be related to a local climate characterised by a high average sky coverage (over 50%), which limits the potential of photovoltaic generation.

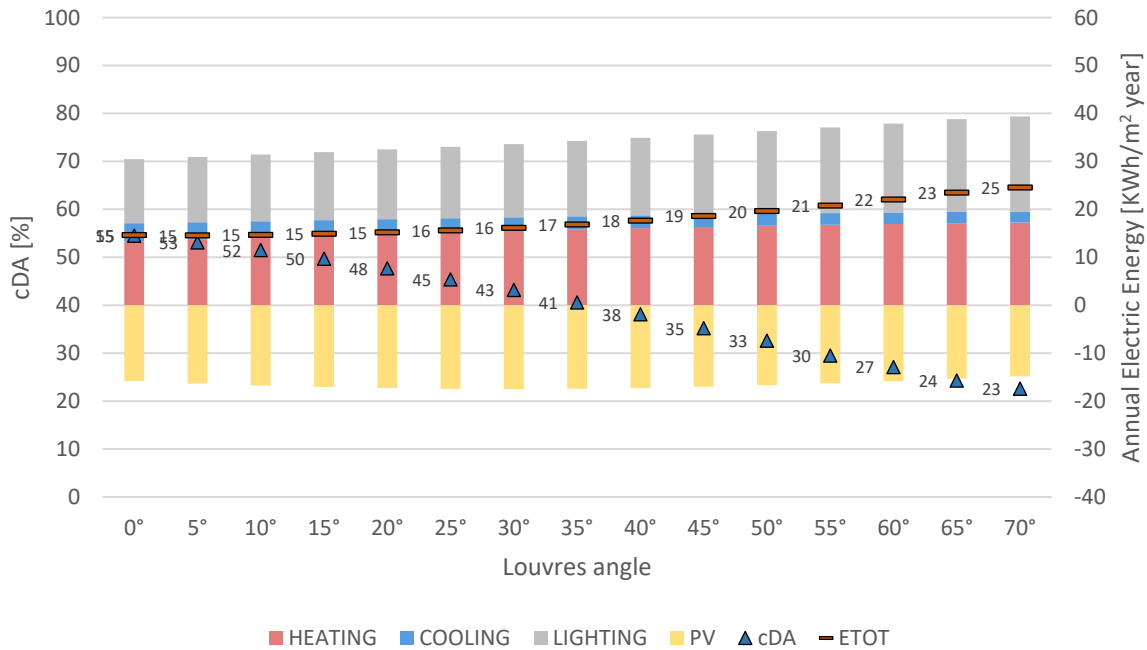


Fig. 190. Chart showing the Brussels share of energy and cDA for the different configurations of the photovoltaic shading devices

The overall energy consumption is lower than in Oslo due to a smaller share of heating demand thanks to a milder climate. In **Fig. 20** is visible how only the first three angles are available to be selected as best fixed configurations, with the optimal one resulting from being the 5°. Having it as reference case, the optimised schedules for different time-steps have been created. Again, a comparison could be made with the Norwegian capital, having here levels of optimisation for the total energy consumption in line with the ones in Oslo, with the same value for the monthly schedule and a slightly better one for the weekly option, as visible in **Table 10**.

Table 10. Overview of the optimisation of a dynamic system over a static one for Brussels

TIME-STEPS	cDA [%]	E _{TOT} [KWh/m ² year]	OPTIMISED cDA	OPTIMISED E _{TOT}
FIX 5°	53.1%	14.6		
SEASONAL	53.1%	14.4	0.0%	1.4%
MONTHLY	51.9%	14.2	-2.3%	2.9%
WEEKLY	52.2%	13.9	-1.7%	4.4%

4.3 Rome

The city of Rome was another one of the main focus of the research. By observing the chart in **Fig. 21** is visible how the energy use and the natural daylight availability is drastically different from the two previous cases. The demand for heating in Rome is relatively low, thanks to the mild climate that characterises the Italian capital for a great part of the year, while the cooling load is significant. The cDA remains high for most of the configurations, dropping under 50% only at 40°. This helps to keep the electric energy consumption for artificial lighting low and have a broader range of selectable options.

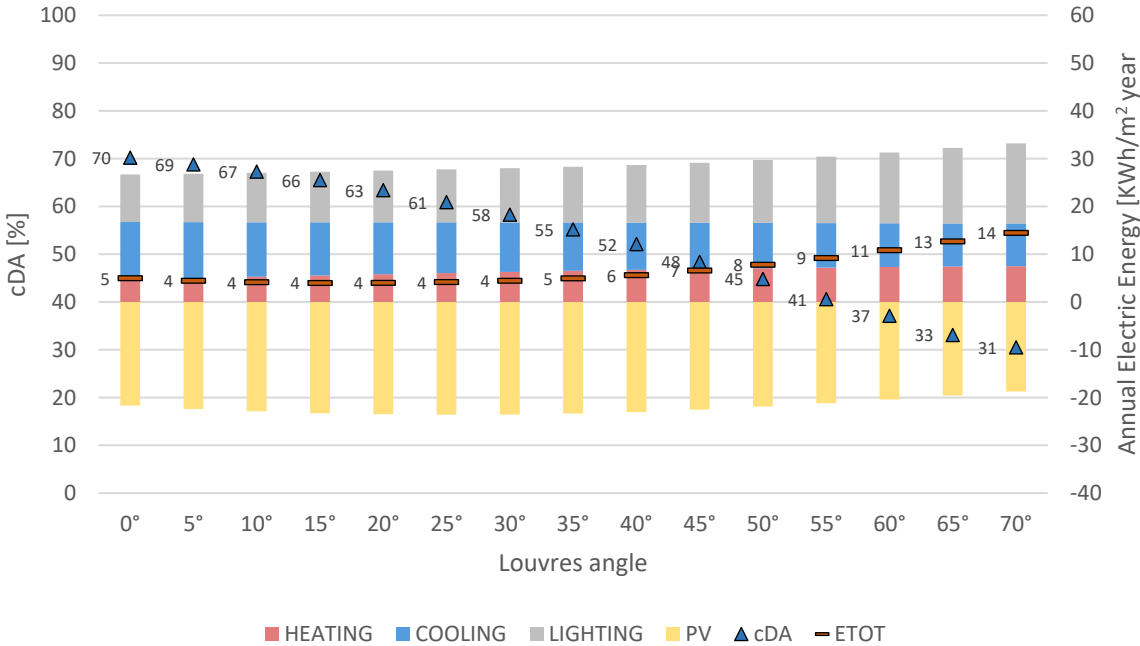


Fig. 201. Chart showing the Rome 16 louvres share of energy and cDA for the different configurations of the photovoltaic shading device

The great difference between the two previous cases is represented by the amount of solar energy harvested by the PV. The electricity produced compensates for a large portion of the energy demand of the building, keeping many of the E_{TOT} values around 4 KWh/m^2 year. The best configuration for a fixed system is here the one at 15°, used as the matter of comparison in building up the optimised schedules. Rome shows significant potential for optimisation, giving encouraging results already with a seasonal schedule, with a 14% improvement over the fixed system. By increasing the frequency of changes to a monthly and weekly base, the numbers become even more promising, with increments close to 20%, while the cDA is kept over a more than acceptable value of 60% (**Table 11**).

Table 11. Overview of the optimisation of a dynamic system over a static one for Rome 16 louvres

TIME-STEPS	cDA [%]	E _{TOT} [KWh/m ² year]	OPTIMISED cDA	OPTIMISED E _{TOT}
FIX 15°	65.5%	4.0		
SEASONAL	64.7%	3.4	-1.2%	14.0%
MONTHLY	64.7%	3.2	-1.2%	18.8%
WEEKLY	64.6%	3.1	-1.4%	21.8%

The better results obtained in Rome compared to Brussels and Oslo have to be attributed mainly to the better PV harvesting and the more important role played by the shading device in shades the building and consequently in reducing the energy for cooling. As the latitude gets lower and the amount of solar radiation increases, adjusting the shading system to follow the sun position and blocking at the same time the unwanted solar radiation gives enhanced performance compared to a fixed solution.

4.3.1 Rome 13 and 10 louvres

Similarly to what done for Oslo, the configurations with 13 and 10 louvres have been tested on seasonal and monthly time-steps. Apart from having a better daylight condition by going for one of these two options, no other advantages are recordable in comparison to the 16 louvres solution. Here more than in Oslo, the loss of louvres does not prove to be convenient in terms of energy-saving, despite the improvement related to the reduction of the self-shading. A minor number of louvres generates in Rome a doubly negative effect, providing not only less electricity from PV (-14% for 13 louvres and -30% for 10 louvres), but also a significant reduction of effectiveness of the system intended as a simple shading device, with higher cooling demand. Although a satisfactory level of optimisation is achievable, a slightly better share of natural daylight over the year does not justify the steep increase in E_{TOT} to values two and almost three times the 16 louvres solution as is visible in **Table 12** below.

Table 12. Overview of optimised results for 13 and 10 louvres configurations in Rome and the percentage difference to the 16 louvres configuration for cDA and E_{tot}

TIME-STEPS	cDA [%]	E _{TOT} [KWh/m ² year]	Δ cDA 16 LOUVRES	Δ E _{TOT} 16 LOUVRES	OPTIMISED cDA	OPTIMISED E _{TOT}
------------	---------	--	------------------	-------------------------------	---------------	----------------------------

13 BLINDS	FIX 25°	65.70%	7.4				
	SEASONAL	65.70%	6.7	1.5%	96.3%	0.00%	8.74%
	MONTHLY	65.70%	6.5	1.5%	101.5%	0.00%	11.55%
10 BLINDS	FIX 30°	68.90%	11.0				
	SEASONAL	68.80%	10.4	6.3%	204.3%	-0.15%	4.98%
	MONTHLY	69.20%	10.3	7.0%	219.1%	0.44%	5.93%

4.4 Cairo

The city of Cairo in Egypt represents the most extreme location among the ones selected for the study. The chart in **Fig. 22** shows the sharp difference in the energy pattern and cDA for fixed configurations, compared to the previous examples. An acceptable level of natural daylight is guaranteed for almost every configuration, actively reducing the need for artificial lighting.

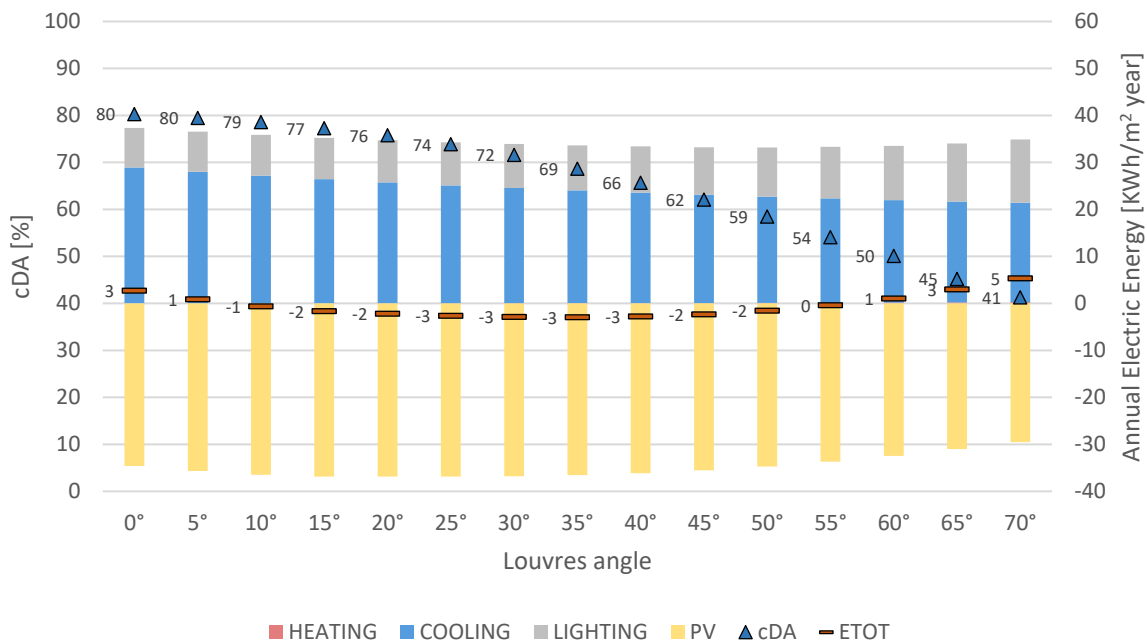


Fig. 212. Chart showing the Cairo 16 louvres share of energy and cDA for the different configurations of the photovoltaic shading device

The heating demand is wholly absent, and the predominant share of energy is required to warm down the building. Cooling accounts for almost all the energy demand, spanning from nearly 30 KWh/m² year when the shading device is fully opened, to 21 KWh/m² year, with 70° angles. Cairo allowed for a high amount of solar energy to be harvested, making it possible for some PVSD configuration to fully compensate the energy needs of the office room, having even additional spare of energy. In Cairo, the best solution for a fixed system composed of 16 louvres

has proven to be the 35°, which is a relatively steep angle in comparison to the ones selected for Oslo, Brussels, and Rome.

Thanks to high levels of cDA, Cairo permits an almost free selection of all the options, a fact reflected in the composition of the optimised dynamic schedules. During summer months, low angles are selected to stop the almost vertical solar radiation and maximise PV generation, while for the rest of the year higher angles are picked, boosting the energy production without compromising the daylight condition. This trend is visible in **Fig. 23**, where a graphical visualisation of the three optimised schedules is presented.

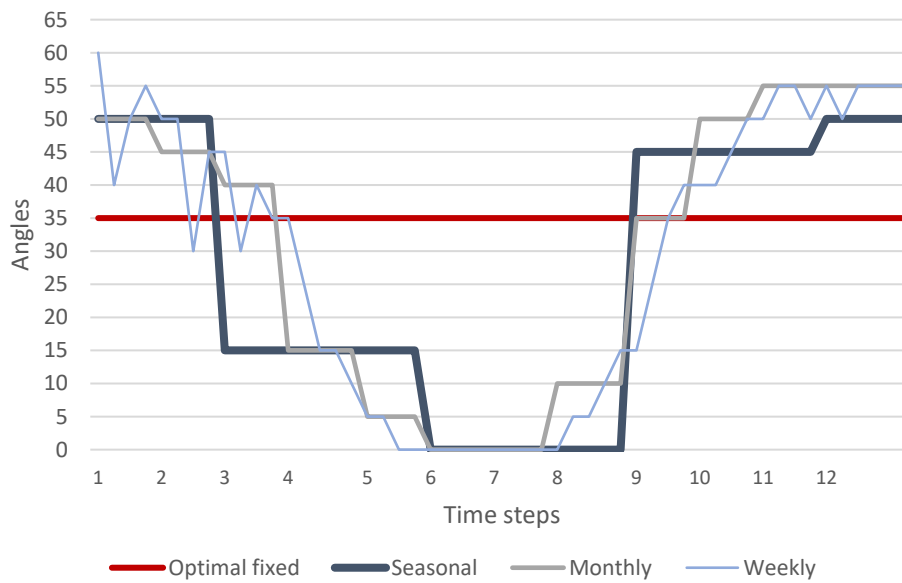


Fig. 23. Chart illustrating angles' alternation for seasonal, monthly, and weekly schedules for Cairo 16 louvres

If compared to Oslo, the behaviour of the dynamic PVSD in Cairo is the opposite, thus leading here to high levels of optimisation (**Table 13**). Already with a seasonal schedule, which implies only four changes in system's orientation over one year, the advantages of having a dynamic system are elevated, leading to an optimisation of more than 83% for the E_{TOT} as well as a small increment in the cDA. Moving to monthly and weekly solutions, the results are even more encouraging, with an efficiency almost doubled.

Table 13. Overview of the optimisation of a dynamic system over a static one for Cairo 16 louvres

TIME-STEPS	cDA [%]	E_{TOT} [KWh/m ² year]	OPTIMISED cDA	OPTIMISED E_{TOT}
FIX 35°	68.7%	-2.9		
SEASONAL	69.4%	-5.4	1.0%	83.6%
MONTHLY	68.1%	-5.8	-0.9%	98.4%
WEEKLY	68.0%	-5.9	-1.0%	101.5%

4.4.1 Cairo 19 louvres

In order to understand if a different number of louvres would have performed better for a similar climate, a 19 blinds option has been tested. The decision to evaluate a system with more louvres was taken after analysing the outputs from lower number configurations in Oslo, and especially Rome. Despite decreasing the louvres lead to an increment of overall cDA with the possibility of choosing more options when composing the dynamic schedules, it also implies a fall in the PV production and a diminishing cooling effect as drawbacks. In a hot climate would have therefore sense to increment the number of louvres to enhance energy production and exploit even more the passive cooling effect of shadows. Although the natural daylight would slightly decrease because of that, in locations like Cairo would still be high enough to guarantee a satisfactory level and a large variety of selectable angles for a dynamic system.

These considerations are reflected in the results, visible in **Table 14**. Seasonal and monthly schedules were tested, resulting in a large amount of net energy produced by the system. The potential for dynamic optimisation is here lower, but still significantly relevant.

Table 14. Overview of the optimisation of a dynamic system over a static one for Cairo 19 louvres

TIME-STEPS	cDA [%]	E _{TOT} [KWh/m ² year]	OPTIMISED cDA	OPTIMISED E _{TOT}
FIX 30°	65.6%	-9.3		
SEASONAL	65.0%	-11.3	-0.9%	21.5%
MONTHLY	65.5%	-11.7	-0.1%	25.8%

4.5 Limitations of the study

In presenting the study's limitation, the first one can be found in the fact that even though several latitudes were investigated, all the settings have been left unchanged. This was primarily done to allow a straight comparison between results, despite it could also be considered a limitation. Taking, for instance, the setpoints temperatures, different values could have been applied according to an adaptive thermal comfort model. In this specific situation, a crucial role is, in fact, played by the ΔT between indoor and outdoor temperatures, together with the presence of natural air drafts.

Another limitation was that glare was not considered as a parameter of the optimisation process, keeping the objective functions of the optimisation to two (E_{TOT} and cDA). However, the

presence of glare can strongly affect the productivity of occupants and is recognised as one of the leading causes of discomfort in indoor environment.

Finally, the lack of automation in the developed process can be seen as one last limitation. Each series of simulations was performed manually by switching every time the settings, activity that has proven to be particularly time-consuming when handling a large amount of data. The thermal history check could have been done much faster in the presence of system automation, giving the chance to explore more solutions or locations instead. The creation of a schedule, able to modify the orientation of louvres on a daily base was also judge impossible to realised due to the same problem.

5 Conclusion

The scope of the research was to assess the advantages of a dynamic photovoltaic shading system over a static one in terms of daylight and total energy consumption, as well as understanding the impact of dynamic change frequency over the year. This was tested at different latitudes and climate zones. Through the study, it was possible to evince that a static system, even in its best possible configuration, has always to be considered as a compromise among several optimal solutions. However, a dynamic system will always perform better than its static counterpart, especially when the changing frequency of the component is increased to better respond to different climatic conditions and sun positions. Despite that, as the results show convincingly, the potential for optimisation varies consistently according to different geographical location.

This fact can be attributed to the nature itself of the component object of the analysis, a shading device with integrated photovoltaic cells. Its main scope is to reduce the cooling load for the building by blocking the unwanted solar radiation and simultaneously converting it into energy. More effectiveness can be obtained in places where a high level of solar radiation is present, and the need for cooling is elevated. This partially explains why at high latitudes as Oslo and Brussels, where low cooling loads are present, and the radiation intensity is not particularly high, the potential for optimisation is limited, while at lower latitudes more satisfactory outputs are visible.

Another critical aspect to consider when evaluating the effectiveness of a dynamic system over a static one is the numbers of louvres. The reduction in louvres to 13 and 10 tested for Oslo and Rome did not correspond to better performance. For locations situated at high latitudes as Oslo, the decrement could potentially be beneficial, allowing the selection of more tilted angles for PV production when creating the dynamic schedules without compromising the daylight. On the contrary, in Rome, reducing the louvres does not generate any advantages having here a daylight condition that already allows the selection of a wide range of optimal angles. For both cases, the worst results are due to the relevant role played by PV in compensating the energy consumption, which is strongly compromised with a decrement in the number of louvres.

A reason to go for a lower number could be the willingness of enhancing the outside view thanks to wider gaps between elements, at the expense of higher energy demand, or the use of LCA as a tool to calculate the emissions related to the component's production and assessed the convenience of it. Despite these are possible aspects to focus on, were not the primary purpose of the actual research and were therefore not investigated. The results collected in Oslo and Rome on the variation of louvres' number were used to test an approach in the opposite direction for Cairo, where a 19 louvres configuration was additionally tested, resulting in a better overall performance. It has been demonstrated that for lower latitudes, a higher number of louvres is desirable to maximise the benefits of shading and PV, even if lower effectiveness of the dynamic optimisation was measured.

In conclusion, it is possible to state that dynamic PVSD systems are performing better than their static counterpart, especially at low latitudes where their potential can be fully exploited. However, a well-design static system could prove to be a good compromise at higher latitudes where the optimisation margin for dynamic systems was proven to be limited, avoiding the complications related to a more complex movable system.

5.1 Further developments

Possible further developments for future investigation on the topic could be summarised as:

1. The development of a Grasshopper definition able to include the automation of the process allowing for a faster optimisation process
2. The introduction of glare as an objective function to consider when selecting angles for the creation of a dynamic schedule
3. The consideration of LCA principles when deciding the numbers of louvres constituting the system, having, in this way, a more comprehensive vision, able to include the energy used during the production and assembly of the component
4. The consideration of economic aspects of different solutions as part of the decisional process for the selection of the best option

Bibliography

- Abdullah, H.K., Alibaba, H.Z., 2017. Retrofits for Energy Efficient Office Buildings: Integration of Optimized Photovoltaics in the Form of Responsive Shading Devices. *Sustainability* 9, 2096. <https://doi.org/10.3390/su9112096>
- Alzoubi, H.H., Al-Zoubi, A.H., 2010. Assessment of building façade performance in terms of daylighting and the associated energy consumption in architectural spaces: Vertical and horizontal shading devices for southern exposure facades. *Energy Convers. Manag.*, Global Conference on Renewables and Energy Efficiency for Desert Regions (GCREEDER 2009) 51, 1592–1599. <https://doi.org/10.1016/j.enconman.2009.08.039>
- Bahr, W., 2014. A comprehensive assessment methodology of the building integrated photovoltaic blind system. *Energy Build.* 82, 703–708. <https://doi.org/10.1016/j.enbuild.2014.07.065>
- Bizzarri, G., Gillott, M., Belpoliti, V., 2011. The potential of semitransparent photovoltaic devices for architectural integration: The development of device performance and improvement of the indoor environmental quality and comfort through case-study application. *Sustain. Cities Soc.* 1, 178–185. <https://doi.org/10.1016/j.scs.2011.07.003>
- Daylighting Pattern Guide, 2020. Daylighting Pattern Guide [WWW Document]. URL <https://patternguide.advancedbuildings.net/using-this-guide/analysis-methods/continuous-daylight-autonomy> (accessed 5.23.20).
- Defaix, P.R., van Sark, W.G.J.H.M., Worrell, E., de Visser, E., 2012. Technical potential for photovoltaics on buildings in the EU-27. *Sol. Energy* 86, 2644–2653. <https://doi.org/10.1016/j.solener.2012.06.007>
- Dolara, A., Lazaroiu, G.C., Leva, S., Manzolini, G., 2013. Experimental investigation of partial shading scenarios on PV (photovoltaic) modules. *Energy* 55, 466–475. <https://doi.org/10.1016/j.energy.2013.04.009>
- Eltaweel, A., Su, Y., 2017. Parametric design and daylighting: A literature review. *Renew. Sustain. Energy Rev.* 73, 1086–1103. <https://doi.org/10.1016/j.rser.2017.02.011>
- Fernandes, L., 2006. Coordinate Systems for Representation of Bidirectional Optical Properties of Fenestration. Lawrence Berkeley National Laboratory, California, USA.
- Frazer, J., 2016. Parametric Computation: History and Future. *Archit. Des.* 86, 18–23. <https://doi.org/10.1002/ad.2019>
- Frontini, F., Bonomo, P., Chatzipanagi, A., 2015. SEAC SUPSI report 2015 BIPV product overview for solar facades and roofs.
- Gao, Y., Dong, J., Isabella, O., Santbergen, R., Tan, H., Zeman, M., Zhang, G., 2018. A photovoltaic window with sun-tracking shading elements towards maximum power generation and non-glare daylighting. *Appl. Energy* 228, 1454–1472.
- Grynberg, A., 1989. Validation of RADIANCE. Lawrence Berkeley Lab. Berkeley LBID 1575.
- Hassan, A., Abdin, A., Ezzeldin, S., 2017. Parallel Parametric Simulation for Optimizing Non-Conventional Solar Screens: An Approach for Balancing Daylight and Thermal Performance in Hot Arid Climates.
- Hensen, J.L.M., Lamberts, R., 2019. Building Performance Simulation for Design and Operation. Routledge.
- Hestnes, A.G., 1999. Building Integration Of Solar Energy Systems. *Sol. Energy* 67, 181–187. [https://doi.org/10.1016/S0038-092X\(00\)00065-7](https://doi.org/10.1016/S0038-092X(00)00065-7)
- Hestnes, A.G., Eik-Nes, N.L., 2017. Zero Emission Buildings. Fagbokforlaget.
- Hong, S., Choi, A.-S., Sung, M., 2017. Development and verification of a slat control method for a bi-directional PV blind. *Appl. Energy* 206, 1321–1333. <https://doi.org/10.1016/j.apenergy.2017.10.009>
- Hong, T., Jeong, K., Koo, C., Kim, J., Lee, M., 2016. A Preliminary Study for Determining Photovoltaic Panel for a Smart Photovoltaic Blind Considering Usability and Constructability Issues. *Energy Procedia*, CUE 2015 - Applied Energy Symposium and Summit 2015: Low carbon cities and urban energy systems 88, 363–367. <https://doi.org/10.1016/j.egypro.2016.06.135>

- Hong, T., Koo, C., Oh, J., Jeong, K., 2017. Nonlinearity analysis of the shading effect on the technical–economic performance of the building-integrated photovoltaic blind. *Appl. Energy* 194, 467–480. <https://doi.org/10.1016/j.apenergy.2016.05.027>
- Ibraheem, Y., PIROOZFAR, P., Farr, E.R., Ravenscroft, N., 2020. Energy production analysis of Photovoltaic Shading Devices (PVSD) in Integrated Façade Systems (IFS). *Front. Built Environ.* 6, 81.
- IEA, 2020. World energy balances (Edition 2019). International Energy Agency.
- IEA, 2018. International definitions of BIPV, Photovoltaic Power System Programme. International Energy Agency.
- Iversen, A., Roy, N., Hvass, M., Jørgensen, M., Christoffersen, J., Osterhous, W., Johnsen, K., 2013. Daylight calculations in practice: An investigation of the ability of nine daylight simulation programs to calculate the daylight factor in five typical rooms.
- Jeong, K., Hong, T., Koo, C., Oh, J., Lee, M., Kim, J., 2017. A Prototype Design and Development of the Smart Photovoltaic System Blind Considering the Photovoltaic Panel, Tracking System, and Monitoring System. *Appl. Sci.* 7, 1077. <https://doi.org/10.3390/app7101077>
- Karkaniyas, C., Boemi, S.N., Papadopoulos, A.M., Tsoutsos, T.D., Karagiannidis, A., 2010. Energy efficiency in the Hellenic building sector: An assessment of the restrictions and perspectives of the market. *Energy Policy, The Role of Trust in Managing Uncertainties in the Transition to a Sustainable Energy Economy, Special Section with Regular Papers* 38, 2776–2784. <https://doi.org/10.1016/j.enpol.2010.01.009>
- Khaing, H.H., Liang, Y.J., Htay, N.N.M., Fan, J., 2014. Characteristics of different solar PV modules under partial shading. *Int J Electr Comput Electron Commun Eng* 8, 1328–1332.
- Kim, J.-J., Jung, S.K., Choi, Y.S., Kim, J.T., 2010. Optimization of Photovoltaic Integrated Shading Devices: Indoor Built Environ. <https://doi.org/10.1177/1420326X09358139>
- Klepeis, N., Nelson, W., Ott, W., Robinson, J., Tsang, A., Switzer, P., Behar, J., Hern, S., Engelmann, W., 2001. The National Human Activity Pattern Survey (NHAPS): A resource for assessing exposure to environmental pollutants. *J. Expo. Anal. Environ. Epidemiol.* 11, 231–52. <https://doi.org/10.1038/sj.jea.7500165>
- Ladybug Tools, 2020. Ladybug Tools [WWW Document]. URL <https://www.ladybug.tools/> (accessed 5.18.20).
- Larson, G.W., Shakespeare, R., 1998. *Rendering with Radiance - The Art and Science of Light Visualization*. Morgan Kaufmann, San Francisco, CA.
- Mandalaki, M., Tsoutsos, T., Papamanolis, N., 2014. Integrated PV in shading systems for Mediterranean countries: Balance between energy production and visual comfort. *Energy Build.* 77, 445–456. <https://doi.org/10.1016/j.enbuild.2014.03.046>
- Mandalaki, M., Zervas, K., Tsoutsos, T., Vazakas, A., 2012. Assessment of fixed shading devices with integrated PV for efficient energy use. *Sol. Energy* 86, 2561–2575. <https://doi.org/10.1016/j.solener.2012.05.026>
- Mardaljevic, J., 2001. The BRE-IDMP dataset: a new benchmark for the validation of illuminance prediction techniques. *Light. Res. Technol.* 33, 117–134. <https://doi.org/10.1177/136578280103300209>
- Mardaljevic, J., 2000. Daylight simulation: validation, sky models and daylight coefficients (thesis). Loughborough University.
- Mardaljevic, J., 1995. Validation of a lighting simulation program under real sky conditions. *Int. J. Light. Res. Technol.* 27, 181–188. <https://doi.org/10.1177/14771535950270040701>
- McNeil, A., 2015. genBSDF Tutorial. Lawrence Berkeley National Laboratory.
- McNeil, A., 2013. The Three-Phase Method for Simulating Complex Fenestration with Radiance. Lawrence Berkeley Natl. Lab.
- McNeil, A., Jonsson, C.J., Appelfeld, D., Ward, G., Lee, E.S., 2013. A validation of a ray-tracing tool used to generate bi-directional scattering distribution functions for complex fenestration systems. *Sol. Energy* 98, 404–414. <https://doi.org/10.1016/j.solener.2013.09.032>
- McNeil, A., Lee, E.S., 2013. A validation of the Radiance three-phase simulation method for modelling annual daylight performance of optically complex fenestration systems. *J. Build. Perform. Simul.* 6, 24–37. <https://doi.org/10.1080/19401493.2012.671852>
- Mitchel, R., Kohler, C., Curcija, D., Zhu, L., Vidanovic, S., Czarnecki, S., Arasteh, D., 2019. WINDOW 7 User Manual. Lawrence Berkeley National Laboratory, California, USA.

- Moretti, L., Mulazzani, M., Bucci, F., 2000. Luigi Moretti: opere e scritti. Electa, Milano.
- Nagy, Z., Svetozarevic, B., Jayathissa, P., Begle, M., Hofer, J., Lydon, G., Willmann, A., Schlueter, A., 2016. The Adaptive Solar Facade: From concept to prototypes. *Front. Archit. Res.* 5, 143–156. <https://doi.org/10.1016/j.foar.2016.03.002>
- Perez, M.J.R., Fthenakis, V., Kim, H.-C., Pereira, A.O., 2012. Façade-integrated photovoltaics: a life cycle and performance assessment case study. *Prog. Photovolt. Res. Appl.* 20, 975–990. <https://doi.org/10.1002/pip.1167>
- Reinhart, C.F., Mardaljevic, J., Rogers, Z., 2006. Dynamic Daylight Performance Metrics for Sustainable Building Design. *LEUKOS* 3, 7–31. <https://doi.org/10.1582/LEUKOS.2006.03.01.001>
- Reinhart, C.F., Walkenhorst, O., 2001. Validation of dynamic RADIANCE-based daylight simulations for a test office with external blinds. *Energy Build.* 33, 683–697. [https://doi.org/10.1016/S0378-7788\(01\)00058-5](https://doi.org/10.1016/S0378-7788(01)00058-5)
- Rogers, Z., 2006. Daylighting Metric Development Using Daylight Autonomy Calculations In the Sensor Placement Optimization Tool. Architecture Energy Corporation, Boulder, Colorado, USA.
- Roudsari, M., 2018. Daylight simulation with Honeybee[+] vs Honeybee Legacy. GitHub. URL <https://github.com/ladybug-tools/honeybee/wiki/Daylight-simulation-with-Honeybee%5B-%5D-vs-Honeybee-Legacy> (accessed 5.22.20).
- Roudsari, M., 2013. Ladybug: a parametric environmental plugin for grasshopper to help designers create an environmentally-conscious design. Presented at the IBPSA Conference, Lyon, France.
- Saxena, M., Ward, G., Perry, T., Heschang, L., Higa, R., 2010. Dynamic Radiance - Predicting annual daylighting with variable fenestration optics using BSDFs. Fourth Natl. Conf. IBPSA-USA.
- SolarGaps, 2020. SolarGaps Smart Blinds with Solar Panels - Renewable Energy Solutions [WWW Document]. Smart Extern. Blinds Sol. Panels - Renew. Energy Solut. URL <https://solargaps.com/> (accessed 6.5.20).
- Subramaniam, S., 2017. Daylighting Simulations with Radiance using Matrix-based Methods. Lawrence Berkeley National Laboratory.
- Taveres-Cachat, E., Bøe, K., Lobaccaro, G., Goia, F., Grynning, S., 2017. Balancing competing parameters in search of optimal configurations for a fix louvre blade system with integrated PV. *Energy Procedia, CISBAT 2017 International Conference Future Buildings & Districts – Energy Efficiency from Nano to Urban Scale* 122, 607–612. <https://doi.org/10.1016/j.egypro.2017.07.357>
- Taveres-Cachat, E., Lobaccaro, G., Goia, F., Chaudhary, G., 2019. A methodology to improve the performance of PV integrated shading devices using multi-objective optimization. *Appl. Energy* 247, 731–744. <https://doi.org/10.1016/j.apenergy.2019.04.033>
- Walker, A., 2013. *Solar Energy: Technologies and Project Delivery for Buildings*. John Wiley & Sons.
- Yoo, S.-H., Lee, E.-T., Lee, J.-K., 1998. BUILDING INTEGRATED PHOTOVOLTAICS: A KOREAN CASE STUDY. *Sol. Energy* 64, 151–161. [https://doi.org/10.1016/S0038-092X\(98\)00115-7](https://doi.org/10.1016/S0038-092X(98)00115-7)
- Zhang, W., Lu, L., Peng, J., 2017. Evaluation of potential benefits of solar photovoltaic shadings in Hong Kong. *Energy* 137, 1152–1158. <https://doi.org/10.1016/j.energy.2017.04.166>
- Zhang, X., 2014. Building performance evaluation of integrated transparent photovoltaic blind system by a virtual testbed, in: Undefined.
- Zhang, X., Lau, S.-K., Lau, S.S.Y., Zhao, Y., 2018. Photovoltaic integrated shading devices (PVSDs): A review. *Sol. Energy* 170, 947–968. <https://doi.org/10.1016/j.solener.2018.05.067>

